14

Active Vibration Absorption and Delayed Feedback Tuning

Nejat Olgac
University of Connecticut

Martin Hosek
University of Connecticut

14.1 Introduction

Vibration absorption has been a very attractive way of removing oscillations from structures under steady harmonic excitations. There are many common engineering applications yielding such undesired oscillations. Helicopter rotor vibration, unbalanced rotating power shafts, bridges under constant speed traffic can be counted as examples. We encounter numerous vibration absorption studies starting as early as the beginning of the 20th century to attenuate these vibrations (Frahm, 1911; den Hartog et al., 1928, 1930, 1938).

The fundamental premise in all of these works is to attach an additional substructure (the absorber) to the primary system in order to suppress its oscillations while it is subject to harmonic excitation with a time varying frequency. A simple answer to this effort appears as "*passive vibration absorber*" as described in most vibration textbooks (Rao, 1995; Thomson, 1988; Inman, 1994.) Figure 14.1a depicts one such configuration. The absorber section is designed such that it reacts to the excitation frequency above much more aggressively than the primary does. This makes the bigger part of the vibratory energy flow into the absorber instead of the primary system. This process complies with the literary meaning of the word 'absorption' of the excitation energy.

Based on the underlying premise there has been strong pursuit of new directions in the field of vibration absorption. A good survey paper to read in this area is (Sun et al., 1995). It covers the highlight topics with detailed discussions and the references on these topics. In this document we wish to overview the current trends in the active vibration absorption research and focus on a few highlight themes with some in-depth discussions.

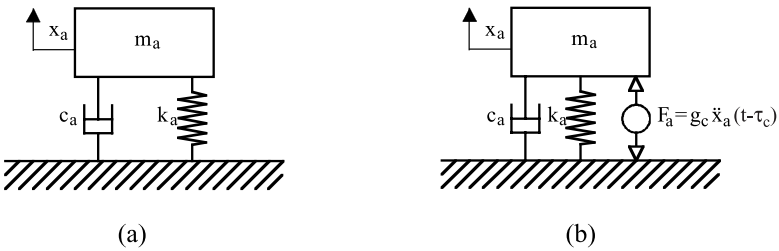

FIGURE 14.1 (a) Mass-spring-damper trio; (b) delayed resonator.

TABLE 14.1 Active Vibration Absorption Research Topics

a. Absorber tuning
1. Active
2. Semi-active
b. Mass ratio minimization
c. Spill-over phenomenon
d. Single and multiple frequency cases, wide-band absorption
e. Stability of controlled systems
f. Novel actuation means

Current research trends in vibration absorption (as displayed in Table 14.1):

- The first and most widely treated topic is the **absorber tuning**. A passive vibration absorber is known to suppress oscillations best in the vicinity of its natural frequencies. This range of effectiveness depends on the specific structural features of the absorber, and it is fixed for a given mechanical structure. Typically, the absorber is harmful, not helpful, outside the mentioned frequency range. That is, the undesired residual oscillations of the system with the absorber are larger in amplitude than those without.
- Can the tuning feature of such passive vibration absorber be improved by adding an active control to the dynamics? This question leads to the main topic of this section: **actively tuned vibration absorbers (ATVA)**. There are numerous methods for achieving active tuning. The format and the particularities of some of these active absorber-tuning methodologies will be covered in this document.

A sub-category of research under "absorber tuning" is semi-active tuning methodology, which is touched upon in two companion sections in this handbook (i.e., Jalili and Valášek). This text focuses on the active tuning methods, only.

- Mass ratio minimization. Most vibration sensitive operations are also weight conscience. Therefore, the application specialists look for minimum weight ratios between the absorber and the primary structure. (Puksand, 1975; Esmailzadeh et al., 1998; Bapat et al., 1979).
- Spill over effect constitutes another critical problem. As the TVA is tuned to suppress oscillations in a frequency interval it should not invoke some undesirable response in the neighboring frequencies. This phenomenon, known as 'spill over effect' needs to be avoided as much as possible (Ezure et al., 1994).
- Single frequency, multiple frequency, and wide-band suppression.

- Stability of the active system.
- New actuators and smart materials. Primarily novel materials (such as piezoelectric and magnetostrictive) are driving the momentum in this field. (See the companion section by Wang.)

Out of these current research topics we focus on (d) and (e) (Table 14.1) in this chapter. In Section 14.2 an ATVA, the delayed resonator (DR) concept is revisited. Both the linear DR and the torsional counterpart, centrifugal delayed resonator (CDR), are considered. The latter also brings about nonlinear dynamics in the analysis. The focus of 14.3 is the multiple frequency DR (MFDR) and the wide-band vibration absorption, also the related optimization work and the stability analysis.

14.2 Delayed Resonator Dynamic Absorbers

The delayed resonator (DR) dynamic absorber is an unconventional vibration control approach which utilizes partial state feedback with time delay as a means of converting a passive mass-spring-damper system into an undamped real-time tunable dynamic absorber.

The core idea of the DR vibration control method is to reconfigure a passive single-degree-of-freedom system (mass-spring-damper trio) so that it behaves like an undamped absorber with a tunable natural frequency. A control force based on proportional partial state feedback with time delay is used to achieve this objective. The use of time delay is what makes this method unique. In contrast to the common tendency to *eliminate* delays in control systems due to their destabilizing effects (Rodellar et al., 1989; Abdel-Mooty and Roorda, 1991), the concept of the DR absorber *introduces* time delay as a tool for pole placement. Despite the vast number of studies on time delay systems available in the literature (Thowsen 1981a, 1981b and 1982; Zitek 1984), its usage for control advantage is rare and limited to stability- and robustness-related issues (Youcef-Toumi et al. 1990, 1991; Yang, 1991).

The delayed control feedback can be implemented using *position, velocity, or acceleration* measurements, depending on the type of sensor selected for a particular vibration control application at hand. In this chapter, acceleration feedback is presented as the core approach, mainly because of exceptional compactness, ruggedness, high sensitivity, and broad frequency range of piezoelectric accelerometers. All these features are essential for high-performance vibration control.

The concept of the tunable DR with absolute position feedback was introduced in Olgac and Holm-Hansen (1994) and Olgac (1995). A single-mass dual-frequency DR absorber was reported in Olgac et al., (1995, 1996) and Olgac (1996). Sacrificing the tuning capability, the single-mass dual-frequency DR absorber can eliminate oscillations at two frequencies simultaneously. As a practical modification of the DR concept, the absolute position feedback was replaced with relative position measurements (relative to the point of attachment of the absorber arrangement) in Olgac and Hosek (1997) and Olgac and Hosek (1995). Delayed acceleration feedback was proposed for high-frequency low-amplitude application in Olgac et al. (1997) and Hosek (1998). The issue of robustness against uncertainties and variations in the parameters of the absorber arrangement was addressed by automatic tuning algorithms presented in Renzulli (1996), Renzulli et al. (1999), and Hosek and Olgac (1999). The DR concept was extended to torsional vibration applications in Filipovic and Olgac (1998), where delayed *velocity* feedback was analyzed, and in Hosek (1997), Hosek et al. (1997a) and (1999a), where synthesis of the delayed control approach with a *centrifugal pendulum absorber* was presented. The concept of the DR absorber was demonstrated experimentally both for the linear and torsional cases in Olgac et al. (1995), Hosek et al. (1997b) and Filipovic and Olgac (1998).

The major contribution of the DR absorber is its ability to eliminate undesired harmonic oscillations with time-varying frequency. Other practical features include small number of operations executed in the control loop (delay and gain), simplicity of implementation (only one or at the most two variables need to be measured), complete decoupling of the control algorithm from the

structural and dynamic properties of the primary system (uncertainties in the model of the primary structure do not affect the performance of the absorber provided that the combined system is stable), and fail tolerant operation (i.e., the feedback control is removed if it introduces instability and passive absorber remains).

In this section, the theoretical fundamentals of DR dynamic absorber are provided, an automatic and robust tuning algorithm is presented against uncertain variations in the mechanical properties. A topic of slightly different flavor, vibration control of rotating mechanical structures via a *centrifugal version of the DR* is also addressed.

The following terminology is used throughout the text: the *primary structure* is the original vibrating machinery alone; the *combined system* is the primary structure equipped with a dynamic absorber arrangement.

14.2.1 The Delayed Resonator Dynamic Absorber with Acceleration Feedback

The delayed feedback for the DR can be implemented in various forms: position (Olgac and Holm-Hansen 1994, Olgac and Hosek 1997), velocity (Filipovic and Olgac 1998) or acceleration (Olgac et al. 1997; Hosek 1998) measurements. The selection is based on the type of sensor that is appropriate for the practical application. In this section, the primary focus is delayed acceleration feedback especially for accelerometer's compactness, wide frequency range, and high sensitivity.

14.2.1.1 Real-Time Tunable Delayed Resonator

The basic mechanical arrangement under consideration is depicted schematically in Figure 14.1. Departing from a passive structure (mass-spring-damper) of Figure 14.1a, a control force F_a between the mass and the grounded base is added for Figure 14.1b. An acceleration feedback control with time delay is utilized in order to modify the dynamics of the passive arrangement:

$$F_a = g\ddot{x}_a(t-\tau) \tag{14.1}$$

where g and τ are the feedback gain and delay, respectively. The equation of motion for the new system and the corresponding (transcendental) characteristic equation are

$$m_a\ddot{x}_a(t) + c_a\dot{x}_a(t) + k_a x_a(t) - g\ddot{x}_a(t-\tau) = 0 \tag{14.2}$$

$$C(s) = m_a s^2 + c_a s + k_a - g s^2 e^{-\tau s} = 0 \tag{14.3}$$

Equation (14.3) possesses infinitely many characteristic roots. When the feedback gain varies from zero to infinity and the time delay is kept constant, these roots move in the complex plane along infinitely many *branches of root loci* (Olgac and Holm-Hansen 1994; Olgac et al. 1997; Hosek 1998).

To achieve pure resonance behavior, two dominant roots of the characteristic Equation (14.3) should be placed on the imaginary axis at the desired resonance frequency ω_c. Introducing this proposition, i.e., $s = \pm\omega_c i$, into Equation (14.3), the following expressions for feedback parameters are obtained*:

$$g_c = \frac{1}{\omega_c^2}\sqrt{\left(c_a\omega_c\right)^2 + \left(k_a - m_a\omega_c{}^2\right)^2} \tag{14.4}$$

*In Equation (14.5) atan2(y,x) is four quadrant arctangent of y and x, $-\pi \le \text{atan2}(y,x) \le +\pi$.

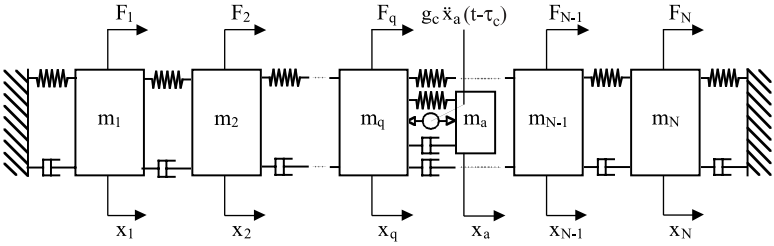

FIGURE 14.2 Schematic of MDOF structure with DR absorber.

$$\tau_c = \frac{\text{atan2}(c_a\omega_c, m_a\omega_c^2 - k_a) + 2(j_c - 1)\pi}{\omega_c}, \quad j_c = 1,2,3,\ldots * \tag{14.5}$$

By this selection of the feedback gain and delay, i.e., $g = g_c$ and $\tau = \tau_c$, the DR can be tuned to the desired frequency ω_c in real time. A complementary set of solutions which gives a negative feedback gain g_c also exists (Filipovic and Olgac 1998). However, for the sake of brevity, it is kept outside the treatment in this text.

The parameter j_c in expression (14.5) refers to the branch of the root loci which is selected to carry the resonant pair of the characteristic roots. While the control gain for a given ω_c remains the same for all branches (Equation 14.4), the values of the feedback delay (Equation 14.5) needed for operation on two consecutive branches of the root loci are related through the following expression:

$$\tau_{c,j_{c+1}} = \tau_{c,j_c} + 2\pi / \omega_c \tag{14.6}$$

The freedom in selecting higher values of j_c becomes a convenient design tool when the DR is coupled to a mechanical structure and employed as a vibration absorber. It allows the designer to relax restrictions on frequencies of operation which typically arise from stability-related issues and due to the presence of an inherent delay in the control loop (Olgac et al. 1997; Filipovic and Olgac 1998; Hosek 1998).

14.2.1.2 Vibration Control of Distributed Parameter Structures

The DR can be coupled to a mechanical structure and employed as a tuned dynamic absorber to suppress the dynamic response at the location of attachment, as depicted schematically in Figure 14.2. When the mechanical structure is subject to a harmonic force disturbance, the DR constitutes an ideal vibration absorber, provided that the control parameters are selected such that the resonance frequency of the DR and the frequency of the external disturbance coincide. The fundamental effect of the absorber is to reduce the amplitude of oscillation of the vibrating system to zero at the location where it is mounted (in this case, m_q).

It is a common engineering practice to represent distributed-parameter systems in a simplified reduced-order form, i.e., using a MDOF model. A typical representation of such a lumped-mass system is shown schematically in Figure 14.2. It consists of N discrete masses m_i which are coupled through spring and damping members and are acted on by harmonic disturbance forces $F_i = A_i \sin(\omega t + \varphi_i)$, $i = 1,2,\ldots,N$. A DR absorber is attached to the q-th mass in order to control oscillations resulting from the disturbance.

*In Equation (14.5) atan2(y,x) is a four-quadrant arctangent of y and x, $-\pi \le \text{atan2}(y,x) \le \pi$.

The dynamic behavior of the primary structure is described by a linear differential equation of motion in conventional form:

$$[M]\{\ddot{x}(t)\}+[C]\{\dot{x}(t)\}+[K]\{x(t)\}=\{F(t)\} \tag{14.7}$$

where [M], [C], and [K] are $N \times N$ mass, damping and stiffness matrices, respectively, {F} is an $N \times 1$ vector of disturbance forces and {x(t)} denotes an $N \times 1$ vector of displacements. Equation (14.7) is represented in the Laplace domain as:

$$[A(s)]\{x(s)\}=\{F(s)\} \tag{14.8}$$

where:

$$[A(s)]=[M]s^2+[C]s+[K] \tag{14.9}$$

With the DR absorber on the q-th mass of the primary structure, Equation (14.9) takes the following form:

$$\left[\tilde{A}(s)\right]\{\tilde{x}(s)\}=\{\tilde{F}(s)\} \tag{14.10}$$

where:

$$\tilde{A}_{i,j}=A_{i,j},\ i,j=1,2,...,N\ \ except\ if\ \ i=j=q \tag{14.11}$$

$$\tilde{A}_{i,N+1}=0,\quad i=1,2,...,q-1\ and\ i=q+1,q+2,...,N \tag{14.12}$$

$$\tilde{A}_{N+1,i}=0,\quad i=1,2,...,q-1\ and\ i=q+1,q+2,...,N \tag{14.13}$$

$$\tilde{A}_{q,q}=A_{q,q}+c_a s+k_a \tag{14.14}$$

$$\tilde{A}_{q,N+1}=-c_a s-k_a+gs^2e^{-\tau s} \tag{14.15}$$

$$\tilde{A}_{N+1,q}=-c_a s-k_a \tag{14.16}$$

$$\tilde{A}_{N+1,N+1}=m_a s^2+c_a s+k_a-gs^2e^{-\tau s} \tag{14.17}$$

$$\tilde{F}_i=F_i,\ i=1,2,...,N \tag{14.18}$$

$$\tilde{F}_{N+1}=0 \tag{14.19}$$

$$\tilde{x}_i=x_i,\ i=1,2,...,N \tag{14.20}$$

$$\tilde{x}_{N+1}=x_a \tag{14.21}$$

The coefficients $A_{i,j}$ are the corresponding elements of the matrix [A] defined in Equation (14.9). Applying Cramer's rule, the displacement of the q-th mass of the primary structure (i.e., the mass where the absorber is located) is obtained as:*

$$x_q(s) = \frac{(m_a s^2 + c_a s + k_a - g s^2 e^{-\tau s}) \det[Q(s)]}{\det[\tilde{A}(s)]} = \frac{C(s) \det[Q(s)]}{\det[\tilde{A}(s)]} \tag{14.22}$$

where:

$$Q_{i,j} = \tilde{A}_{i,j} = A_{i,j}, \; i = 1,2,...,N, \quad j = 1,2,...,N \;\; except \; if \;\; j = q \tag{14.23}$$

$$Q_{i,q} = \tilde{F}_i = F_i, \quad i = 1,2,...,N \tag{14.24}$$

The factor $C(s)$ in the numerator is identical to the characteristic expression of Equation (14.3). Therefore, as long as the absorber is tuned to the frequency of disturbance, i.e., $\omega = \omega_c$, $g = g_c$, $\tau = \tau_c$, the expression for $x_q(\omega i)$ is zero. That is, provided that the denominator of Equation (14.22) possesses stable roots, the primary structure exhibits no oscillatory motion in the steady state:

$$\lim_{t \to \infty} x_q(t) = 0 \tag{14.25}$$

The frequency of disturbance, which is essential information for proper tuning of the DR absorber (see Equations 14.4 and 14.5), can be extracted from the acceleration of the absorber mass. Note that the frequency can be traced in this signal even when the primary structure has been quieted substantially by the DR absorber.

In summary, for the frequency of disturbance ω which agrees with the resonant frequency ω_c, the point of attachment of the absorber comes to quiescence. If the disturbance contains more than one frequency component, such as in the case of a square wave excitation, the delayed absorber is capable of eliminating any single frequency component selected (typically the fundamental frequency), as demonstrated in 14.2.1.6.

14.2.1.3 Stability Analysis of the Combined System

The DR absorber can track changes in the frequency of oscillation as explained above. In the meantime, the stability of the combined system should be assured for all the operating frequencies. We will see that this constraint plays a very critical role in the deployment of DR absorbers.

Stability is a critical issue in any feedback control. A system is said to have bounded-input-bounded-output (BIBO) stability if every bounded input results in a bounded output. A linear time-invariant system is BIBO stable if and only if all of the characteristic roots have negative real parts (e.g., Franklin et al. 1994).

In the following study, the objective is to explore stability properties of the combined system which comprises a multi-degree-of-freedom (MDOF) primary structure with the DR absorber, as depicted diagrammatically in Figure 14.2. It is stressed that the dynamics of the combined system is not related directly to the stability properties of the DR alone. That is, a substantially stable combined system can be achieved despite the fact that the absorber itself operates in a marginally stable mode.

*Abusing the notation slightly, $x_q(s)$ is written for the Laplace transform of $x_q(t)$.

14.2.1.3.1 Characteristic Equation

As explained in 14.2.1.2, the combined system including a reduced-order (MDOF) model of the primary structure and a DR absorber (Figure 14.2) can be represented in the Laplace domain by the following system of equations:

$$\left[\tilde{A}(s)\right]\left\{\tilde{x}(s)\right\} = \left\{\tilde{F}(s)\right\} \tag{14.26}$$

The characteristic equation of the system of Equation (14.26) is identified as $\det[\tilde{A}(s)] = 0$. This determinant can be written out as:

$$[p(s) - gs^2 e^{-\tau s}]\det[P(s)] - [r(s) - gs^2 e^{-\tau s}]\det[R(s)] = 0 \tag{14.27}$$

where:

$$p(s) = m_a s^2 + c_a s + k_a \tag{14.28}$$

$$r(s) = c_a s + k_a \tag{14.29}$$

$$P_{i,j} = \tilde{A}_{i,j}, \quad i,j = 1,2,...,N \tag{14.30}$$

$$R_{i,j} = (-1)^{q+N+1}\tilde{A}_{i,j}, \; i = 1,2,...,q-1, \; j = 1,2,...,N \tag{14.31}$$

$$R_{i,j} = (-1)^{q+N+1}\tilde{A}_{i+1,j}, \; i = q,q+1,...,N, \; j = 1,2,...,N \tag{14.32}$$

For the sake of simplicity in formulation, the characteristic Equation (14.27) is manipulated into the following form:

$$CE(s) = A(s) - B(s)gs^2 e^{-\tau s} = 0 \tag{14.33}$$

where:

$$A(s) = p(s)\det[P(s)] - r(s)\det[R(s)] \tag{14.34}$$

$$B(s) = \det[P(s)] - \det[R(s)] \tag{14.35}$$

The characteristic Equation (14.33) is transcendental and possesses an infinite number of roots, all of which must have negative real parts (i.e., must stay in the left half of the complex plane) for stable behavior of the combined system. Since the number of the roots is not finite, their location must be explored without actually solving the characteristic equation. The well-known argument principle (e.g., Franklin et al. 1994) can be used for this purpose. However, this method requires repeated contour evaluations of the left hand side of the characteristic Equation (14.33) for every frequency of operation, which proves to be computationally demanding and inefficient. In the following section, an alternative method capable of revealing stability zones directly with less computational effort is explained.

14.2.1.3.2 Stability Chart Method

It can be shown that increasing control gain for a given feedback delay leads to instability of the combined system (Olgac and Holm-Hansen 1995a; Olgac et al. 1997). As a direct consequence, the following condition for stable operation of the DR absorber can be formulated: *the gain for*

the absorber control should always remain smaller than the gain for which the combined system becomes unstable. The feedback gain and delay which lead to marginal stability of the combined system are to be determined from the characteristic Equation (14.33).

At the point where the root loci cross from the stable left half plane to the unstable right half plane, there are at least two characteristic roots on the imaginary axis, i.e., $s = \pm\omega_{cs} i$. Imposing this condition in Equation (14.33) yields:

$$g_{cs} = \frac{1}{\omega_{cs}^2} \left| \frac{A(\omega_{cs} i)}{B(\omega_{cs} i)} \right| \tag{14.36}$$

$$\tau_{cs} = \frac{1}{\omega_{cs}} \left[(2j_{cs} - 1)\pi + \angle \frac{A(\omega_{cs} i)}{B(\omega_{cs} i)} \right], j_{cs} = 1, 2, 3, \ldots \tag{14.37}$$

For a given $\tau_c = \tau_{cs}$ the inequality of $g_c < g_{cs}$ should be satisfied for stable operation. In order to visualize this condition, it is convenient to construct superposed parametric plots of $g_c(\omega_c)$ vs. $\tau_c(\omega_c)$ and $g_{cs}(\omega_{cs})$ vs. $\tau_{cs}(\omega_{cs})$ for the DR alone and the combined system, respectively. An example plot is shown and discussed in 14.2.1.5.

14.2.1.4 Transient Time Analysis

Once the stability of the combined system is assured, the transient behavior becomes another question of interest. It determines the time it takes the primary structure to reach a new steady state, i.e., the time needed for the absorption to take effect when any frequency change in the external disturbance occurs. The transient behavior also plays an important role in determination of the shortest allowable time between two consecutive updates of the feedback gain and delay when the absorber tunes to a different frequency. In general, the combined system must be allowed to settle before a new set of the control parameters is applied.

The settling time of the combined system is dictated by the dominant roots (i.e., the roots closest to the imaginary axis) of the characteristic Equation (14.33). Recalling that this equation has infinitely many solutions, a method is needed which determines the distance of the dominant roots from the imaginary axis, $|\alpha|$, without actually solving the equation. The argument principle can be utilized for this purpose (Olgac and Holm-Hansen 1995b; Olgac and Hosek 1997). The corresponding time constant is then obtained as the reciprocal value of $|\alpha|$, and the settling time for the combined system is estimated as four time constants:

$$t_s = 4 / |\alpha| \tag{14.38}$$

Based on the settling time analysis, the time interval is determined between two consecutive modifications of the control parameters. These modifications can take place periodically to track changes in the frequency of operation ω. The time period should always be longer than the corresponding transient response in order to allow the system to settle after the previous update of the control parameters.

14.2.1.5 Vibration Control of a 3DOF System

A three-degree-of-freedom (3DOF) primary structure with a DR absorber in the configuration of Figure 14.2 is selected as an example case. The primary structure consists of a trio of lumped masses m_i (0.6 kg each), which are connected through linear springs k_i (1.7×10^7 N/m each), damping members c_i (4.5×10^2 kg/s each) and acted on by disturbance forces F_i, i = 1, 2, 3. A DR absorber with acceleration feedback is implemented on the mass located in the middle of the system. The structural parameters of the absorber arrangement are defined as $m_a = 0.183$ kg, $k_a = 1.013 \times 10^7$ N/m, and $c_a = 62.25$ kg/s.

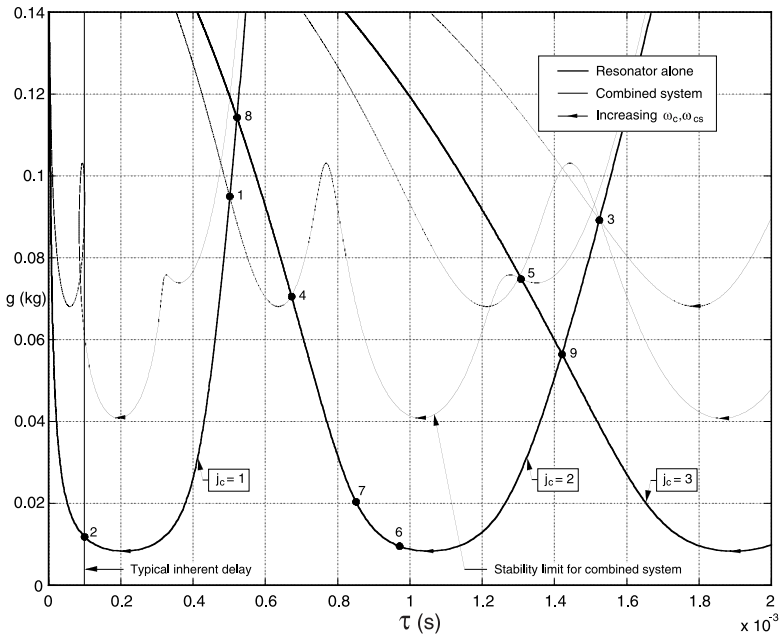

FIGURE 14.3 Plots of $g_c(\omega_c)$ vs. $\tau_c(\omega_c)$ and $g_{cs}(\omega_{cs})$ vs. $\tau_{cs}(\omega_{cs})$.

A stability chart for the example system is shown in Figure 14.3. It consists of superposed parametric plots of $g_c(\omega_c)$ vs. $\tau_c(\omega_c)$ and $g_{cs}(\omega_{cs})$ vs. $\tau_{cs}(\omega_{cs})$ constructed according to Equations (14.4), (14.5) and Equations (14.36), (14.37), respectively. As explained in 14.2.1.3, for a given $\tau_c = \tau_{cs}$ the inequality of $g_c < g_{cs}$ should be satisfied for stable operation. For operation on the first branch of the root loci, this condition is satisfied to the left of point 1. The corresponding operable range is $\tau < \tau_{cr}$ with the critical time delay $\tau_{cr} = 0.502 \times 10^{-3}$ s. In terms of frequency, the stable zone is defined as $\omega_c > \omega_{cr}$ with the lower bound at $\omega_{cr} = 962$ Hz. The upper frequency bound at point 2 results from the presence of an inherent delay in the control loop. For instance, a loop delay of 1×10^{-4} s limits the range of operation on the first branch to 1212 Hz. For the second branch of the root loci, the inequality of $g_c < g_{cs}$ is satisfied between points 3 and 4 in Figure 14.3, that is, for $0.672 \times 10^{-3}\,\text{s} < \tau < 1.524 \times 10^{-3}\,\text{s}$. The corresponding frequency range is found as $972\ \text{Hz} < \omega_c < 1{,}510$ Hz. The upper limit of operation on the third branch is represented by point 5 and corresponds to the frequency of 1530 Hz.

It is observed that operation on higher branches of the root loci introduces design flexibility which can increase operating range of the absorber and improve stability of the combined system. The stability limits can be built into the control algorithm to assure operation only in the stable range. As a preferred alternative, this scheme can be utilized to design the DR absorber with the stability limits desirably relaxed, so that the expected frequencies of disturbance remain operable.

Points 8 and 9 in Figure 14.3 indicate that there are two pairs of characteristic roots of the DR on the imaginary axis simultaneously. Therefore, the DR exhibits two distinct natural frequencies, and can suppress vibration at two frequencies at the same time. This situation is referred to as the **dual frequency fixed delayed resonator** (DFFDR) in the literature (Olgac et al. 1996; Olgac and Hosek 1995; Olgac et al. 1997). Point 8 corresponds to simultaneous operation of the absorber on the 1st and 2nd branches of the root loci. This point is unstable according to the stability chart. Point 9, on the other hand, represents a stable dual-frequency absorber created on the second and third branches of the root loci.

In order to illustrate the real-time tuning ability of the DR absorber, a simulated response of the example system to a step change in the frequency of disturbance is presented in Figure 14.4. Initially,

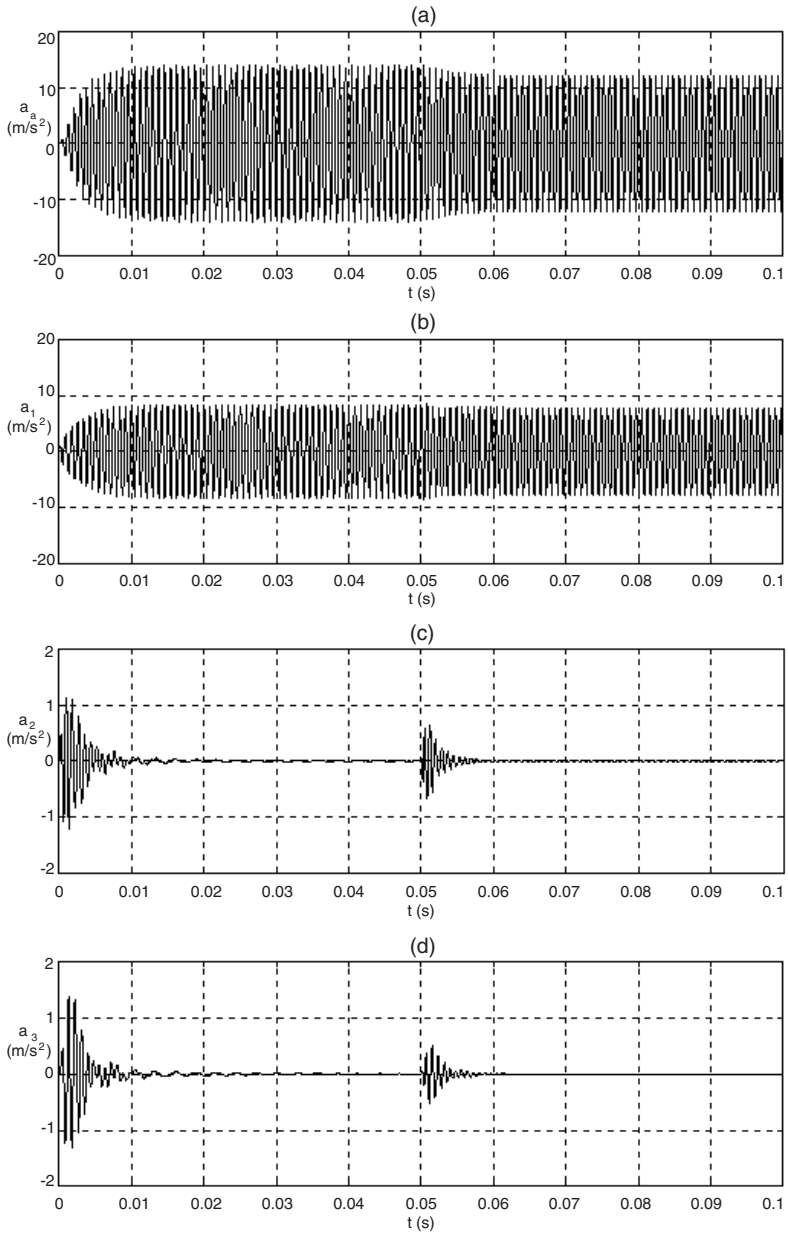

FIGURE 14.4 Simulated response to frequency change from 1200 Hz to 1250 Hz. (a) Absorber, (b) mass 1, (c) mass 2, and (d) mass 3.

a disturbance force in the form of $F_1 = A_1 \sin \omega t$ is applied to mass 1. The amplitude and frequency of disturbance are selected as $A_1 = 1$ N and $\omega = 1200$ Hz, respectively. The corresponding control parameters for the second branch of the root loci are determined as $g_c = 9.55 \times 10^{-3}$ kg and $\tau_c = 0.972 \times 10^{-3}$ s (see point 6 in Figure 14.3). After a short transient period, all undesired oscillations are substantially removed from elements 2 and 3 while mass 1, which is acted on by the disturbance force, keeps vibrating. In other words, the DR absorber creates an artificial node at mass 2, and isolates mass 3 from oscillations at mass 1. At the time t = 0.05 s, a step change in the frequency

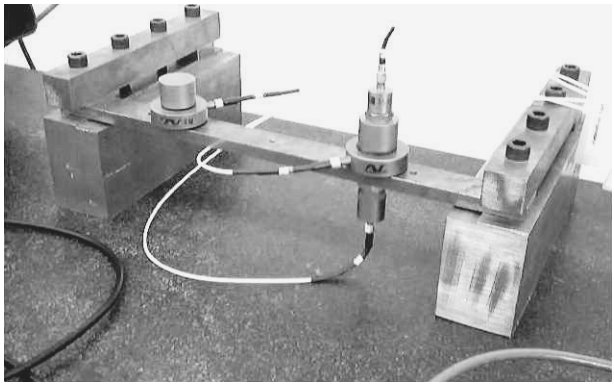

FIGURE 14.5a Experimental set-up.

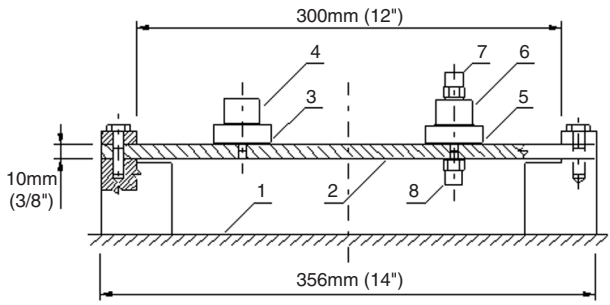

FIGURE 14.5b Side view of the test structure.

of disturbance takes place from 1200 Hz to 1250 Hz. The absorber is retuned accordingly by setting the feedback parameters to $g_c = 2.04 \times 10^{-2}$ kg and $\tau_c = 0.851 \times 10^{-3}$ s (see point 7 in Figure 14.3). After another transient period of approximately the same duration, the vibration suppression comes again into effect and elements 2 and 3 are quieted completely. In short, the DR absorber is capable of eliminating harmonic oscillations at different frequencies at the location where it is attached to the primary structure.

14.2.1.6 Vibration Control of a Flexible Beam

Implementation of the DR dynamic absorber for distributed parameter structures is illustrated by vibration control of a clamped-clamped flexible beam. The test structure is depicted in Figure 14.5a. A side view is detailed in Figure 14.5b. The setup is built on a heavy granite bed (1) which represents the ground. The primary system is selected as a steel beam (2) clamped at both ends. The dimensions of the beam are as follows (height × width × effective length): 10 mm × 25 mm × 300 mm or 3/8" × 1" × 12". A piezoelectric actuator (3) with a reaction mass (4) is mounted on the beam to generate excitation forces. The absorber arrangement comprises another piezoelectric actuator (5) with a reaction mass (6). In this particular case, the structural parameters of the absorber section are identified as $m_a = 0.183$ kg, $k_a = 9.691 \times 10^6$ N/m, and $c_a = 1.032 \times 10^2$ kg/s. The exciter and absorber actuators are located symmetrically at one quarter of the length of the beam from the center. A piezoelectric accelerometer (7) is mounted on the absorber mass (6) to provide signal for the feedback control. Another piezoelectric accelerometer (8) is attached to the beam at the base of the absorber to provide measurements for the automatic tuning algorithm (as described in 14.2) and to monitor vibration of the beam for evaluation purposes. A reduced-order lumped-parameter model of the test structure and the corresponding theoretical and experimental stability charts can

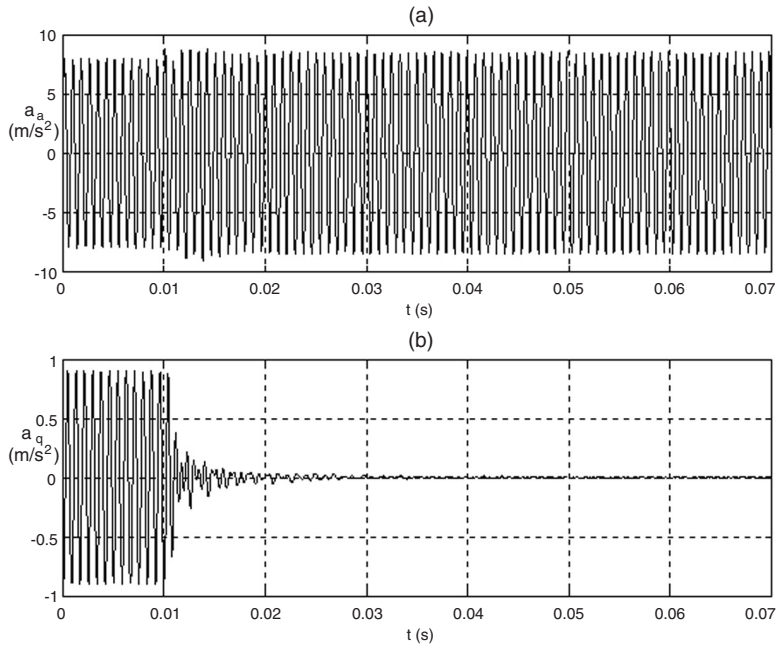

FIGURE 14.6 Time response to a harmonic disturbance at 1200 Hz, branch 2. (a) Acceleration of the absorber, (b) acceleration of the beam.

be found in Olgac et al. (1997). An alternative modal analysis approach is presented in Olgac and Jalili (1998).

In order to demonstrate the DR vibration control concept, a harmonic disturbance at 1200 Hz is applied. The corresponding feedback parameters for operation on the second branch of the root loci are found as $g_c = 1.92 \times 10^{-2}$ kg and $\tau_c = 0.939 \times 10^{-3}$ s. The corresponding time response is shown in Figure 14.6. The diagrams (a) and (b) represent plots of acceleration of the absorber mass (a_a) and acceleration of the beam at the absorber base (a_q), respectively. The control feedback is disconnected for the first 1×10^{-2} s of the test. After its activation, the amplitude of oscillation of the beam is reduced to the level of noise in the signal. The degree of vibration suppression is visualized in the DFT (discrete Fourier transformation) of the steady-state response, as depicted in Figure 14.7. The scale on the vertical axis is normalized with respect to the maximum magnitude of $a_q(\omega i)$, i.e., the ratio of $|a_q(\omega i)| / \max|a_q(\omega i)|$ expressed in percents is shown in the figure. The light line represents the DFT of the steady-state response of the beam with the control feedback disconnected. The bold line depicts the DFT when the control is active. It is observed that the oscillations of the primary structure at the point of attachment of the absorber are reduced by more than 99%.

The test is repeated with a square wave disturbance of the same fundamental frequency, i.e., 1200 Hz. The DFT of the steady-state response of the beam is depicted in Figure 14.8. Again, the ratio of $|a_q(\omega i)| / \max|a_q(\omega i)|$ expressed in percents is used on the vertical axis of the plot. The light line represents the response of the beam with the control feedback disconnected. The bold line is the response with the control active. It is observed that the dominant frequency component of 1200 Hz is suppressed by more than 99% again, while the rest of the frequency spectrum remains practically unchanged. That means no noticeable spill over effect is observed during the absorption.

The real-time tuning capability of the DR dynamic absorber is demonstrated in 14.2, where the beam is subject to a swept-frequency harmonic signal excitation from 650 to 750 Hz at the rate of 2.4 and 10 Hz/s.

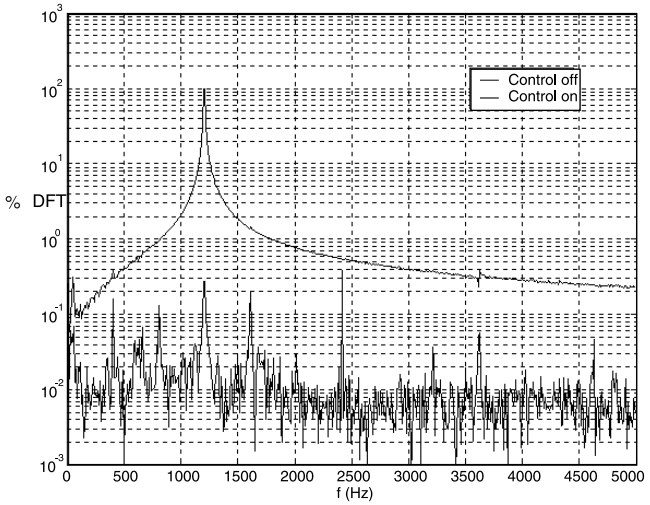

FIGURE 14.7 DFT of the beam response to a harmonic disturbance at 1200 Hz.

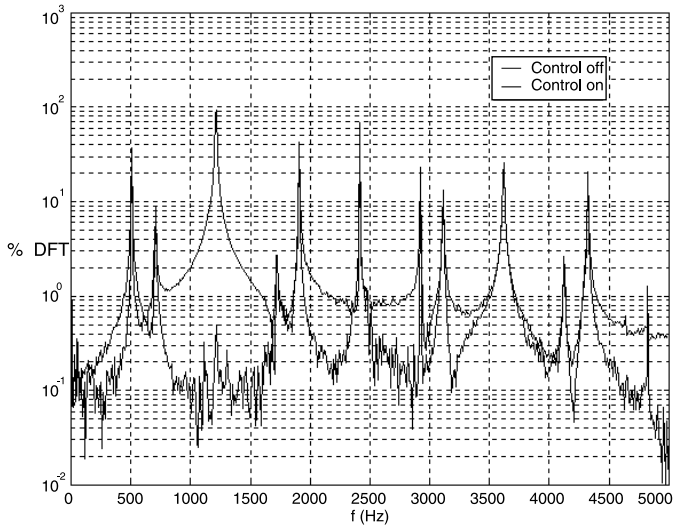

FIGURE 14.8 DFT of the beam response to a square-wave disturbance at 1200 Hz.

14.2.1.7 Summary

The delayed resonator (DR) is an active vibration control approach which utilizes partial state feedback with time delay as a means of converting a passive mass-spring-damper system into an ideal undamped real-time tunable dynamic absorber. The real-time tuning capability and complete suppression of harmonic oscillations at the point of attachment on the primary structure are not the only advantages of the DR absorber. Other practical features that can be found attractive in industrial applications are summarized below.

The frequency of disturbance can be detected conveniently from acceleration of the absorber mass. The feedback gain and delay are functions of the absorber parameters and the operating frequency only (see Equations 14.4 and 14.5). Therefore, the control is entirely decoupled from

the dynamic and structural properties of the primary system. As such, it is insensitive to uncertainties and variations in the primary structure parameters, provided that the combined system remains stable.

Recalling Equation (14.5) and Figure 14.6, higher branches of the root loci can be used to tune the absorber to a given frequency ω_c. This freedom can be considered as a convenient design tool. If the feedback loop contains an inherent time delay, the designer is free to select a higher branch number and increase the required value of τ_c above the inherent delay in the loop. Proper selection of the branch of operation can also improve stability margin and transient response of the combined system (Hosek 1998).

Other practical features of the DR absorber include computational simplicity and fail-safe operation. Due to the simple structure of the feedback, a relatively small number of operations are performed within the control loop. This is particularly important in high-frequency applications where short sampling intervals are required. When the control system fails to operate and/or the feedback is disconnected, the device turns itself into a passive absorber with partial effectiveness, which is considered as a fail-safe feature.

14.2.2 Automatic Tuning Algorithm for the Delayed Resonator Absorber

Real mechanical structures tend to vary their physical properties with time. In particular, the damping and stiffness characteristics involved in their mathematical models often differ from the nominal values. As a natural consequence, insensitivity of the DR absorber performance to parameter variations and uncertainties is an essential requirement in practical applications.

Consider the combined system of a MDOF primary structure with the DR absorber as depicted in Figure 14.2. The Laplace transform of the displacement at the point of attachment of the absorber is in the form:*

$$x_q(s) = \frac{(m_a s^2 + c_a s + k_a - g s^2 e^{-\tau s}) \det[Q(s)]}{\det[\tilde{A}(s)]} \tag{14.39}$$

where the matrices $[Q(s)]$ and $[\tilde{A}(s)]$ are defined in Section 14.2.1.2. Assuming that the roots of the denominator assure stable dynamics for the combined system, the expression in the numerator must vanish for $s = \omega_c i$ in order to achieve zero steady-state response of the q-th element of the primary structure at the frequency $\omega = \omega_c$. Based on this proposition, the control parameters g and τ should be set as:

$$g_c = \frac{1}{\omega_c^2} \sqrt{(c_a \omega_c)^2 + (m_a \omega_c^2 - k_a)^2} \tag{14.40}$$

$$\tau_c = \frac{\operatorname{atan2}(c_a \omega_c, m_a \omega_c^2 - k_a) + 2(j_c - 1)\pi}{\omega_c}, \quad j_c = 1, 2, 3, \ldots \tag{14.41}$$

Equations (14.40) and (14.41) indicate that the control parameters depend on the mechanical properties of the absorber substructure and the frequency of disturbance only. That is, the performance of the DR absorber is insensitive to uncertainties in the parameters of the primary structure, as long as the combined system is stable (stability of the combined system is addressed separately in Section 14.2.1.3).

*Abusing the notation slightly, $x_q(s)$ is written for the Laplace transform of $x_q(t)$.

Insensitivity to uncertainties in the parameters of the primary structure, however, does not guarantee sufficient robustness of the control algorithm. As mentioned earlier, some of the absorber parameters involved in Equations (14.40) and (14.41) are also likely to be contaminated by uncertainties. While the mass m_a can be determined quite accurately and typically does not change its value in time, the other parameters often exhibit undesirable fluctuations. The effective value of the stiffness k_a may depend, for instance, on the amplitude of oscillation of the absorber, and the damping coefficient c_a may be a function of the frequency of operation ω_c. Both of the parameters may also vary with other external factors, such as the temperature of the environment. Due to these uncertainties the actual values of the variables c_a and k_a are not available, and the control parameters g and τ can be set only according to estimated values of c_a and k_a in practice.

Two methods to improve robustness of the control algorithm against such parameter variations and uncertainties have been developed: a single-step automatic tuning algorithm based on on-line parameter identification of the absorber structural properties (Hosek 1998; Hosek and Olgac 1999), and a more general iterative approach which utilizes a gradient method for a direct search for satisfactory values of the control parameters (Renzulli 1996; Renzulli et al. 1999).

The key idea in the single-step approach is to apply control parameters based on the best estimates of the absorber properties available, evaluate the performance achieved, identify the actual mechanical properties of the absorber, calculate the corresponding control parameters, and utilize them in the feedback law. The parameter identification is achieved using the acceleration measurements taken at the absorber's mass and base. The process results in the estimates of two uncertain parameters, c_a and k_a. Details of the single-step automatic tuning algorithm can be found in Hosek (1998) and Hosek and Olgac (1999).

The more universal iterative approach (Renzulli 1996; Renzulli et al. 1998) is selected for presentation in this section. The procedure requires the initial g and τ to be in the vicinity of their actual values. Such a close starting point may be obtained by using the nominal, albeit imperfect, model of the absorber. The tuning process is accomplished through a gradient search method which iteratively converges to the desired values. The analytical formulation of the strategy is discussed first, and is then illustrated by vibration control of a flexible beam subject to swept-frequency excitation.

14.2.2.1 Iterative Automatic Tuning Algorithm

The dynamics of the DR section of the combined system in Laplace domain is given as:

$$(m_a s^2 + c_a s + k_a)x_a(s) + gs^2 e^{-\tau s} x_a(s) = (c_a s + k_a)x_q(s) \tag{14.42}$$

where $x_q(s)$ corresponds to the motion of the base of the absorber and $x_a(s)$ to the motion of the absorber proof mass. This equation can be rewritten as a transfer function between $x_q(s)$ and $x_a(s)$ as:

$$TF = \frac{x_q(s)}{x_a(s)} = \frac{m_a s^2 + c_a s + k_a + gs^2 e^{-\tau s}}{c_a s + k_a}. \tag{14.43}$$

Per Equation (14.39), $x_q(\omega i)$ should be zero if all the structural parameters are perfectly known, and g and τ are calculated as per Equations (14.40) and (14.41). When the parameters k_a and c_a vary, these control parameters must be readjusted for tuning the DR. Otherwise the point of attachment exhibits undesirable oscillations at ω. As a remedy, an adaptation law for the two control parameters, g and τ, is developed.

Before presenting the strategy, two points should be highlighted. First, the fundamental frequency, ω, is observed from the time trace of $\ddot{x}_a(t)$. Second, the ratio

$$\frac{x_q(\omega i)}{x_a(\omega i)} = \frac{\ddot{x}_q(\omega i)}{\ddot{x}_a(\omega i)} = TF(\omega i) \tag{14.44}$$

can be evaluated in real time using the knowledge of ω. The resulting value of $TF(\omega i)$ is the frequency response of the system evaluated at the frequency ω. This is obtained by monitoring the accelerometer readings of $\ddot{x}_a$ and $\ddot{x}_q$, and convolving the time series of these two signals. An extended explanation of the steps involved is given in Renzulli (1996) and Renzulli et al. (1999). As demonstrated there, the convolution imposes minimal computational load when it is done progressively once at each sampling instant.

Assuming that the complex value of the transfer function TF(ωi) is known at ω, a tuning process for g and τ is presented next. Equation (14.43) can be rewritten for $s = \omega i$ as

$$TF(\omega i) = \frac{c_1(\omega i) - g\omega^2 e^{-\tau\omega i}}{c_2(\omega i)} \tag{14.45}$$

where $c_1(\omega i)$ and $c_2(\omega i)$ are complex numbers the nominal values of which are known only.

It is assumed that g and τ can be updated much faster than the speed of variations in c_a and k_a. This is a realistic assumption in most practical applications since the stiffness and damping values typically change gradually. Another assumption is that the absorber structure is capable of tuning itself to the changes in the excitation frequency ω much faster than they occur. These assumptions can be summarized as follows: rate of variations in c_a and k_a << rate of change in ω << sampling speed of g and τ. Consequently, during the robust tuning transition, c_a, k_a, and ω can be considered as constants, though unknown. A variational form of Equation (14.45) then can be written as:

$$\Delta TF(\omega i) = \frac{\partial TF}{\partial g}\Delta g + \frac{\partial TF}{\partial \tau}\Delta\tau + higher\,order\,terms\Big|_{s=\omega i} \tag{14.46}$$

where $\Delta TF(\omega i)$ is the complex variation of $TF(\omega i)$ due to the changes in g and τ (from their respective nominal values). These changes should preferably result in

$$\Delta TF(\omega i) = -TF(\omega i) \tag{14.47}$$

so that the new $TF(\omega i) + \Delta TF(\omega i) = 0$. Assuming that $TF(\omega i) \in C^{\infty}$, and Δg and $\Delta\tau$ are small, the higher order terms in Equation (14.46) can be ignored. This is a reasonable assumption since Δg and $\Delta\tau$ represent differences between the control parameters associated with the nominal values and the true values of k_a and c_a, which are expected to be close numbers. Evaluating the nominal values of the partial derivatives using Equation (14.43),

$$\left.\frac{\partial TF}{\partial g}\right|_{s=\omega i} = -\frac{\omega^2 e^{-\tau\omega i}}{c_a\omega i + k_a} \tag{14.48}$$

$$\left.\frac{\partial TF}{\partial \tau}\right|_{s=\omega i} = -\omega g i \left.\frac{\partial TF}{\partial g}\right|_{s=\omega i} = \frac{\omega^3 i g e^{-\tau\omega i}}{c_a\omega i + k_a}, \tag{14.49}$$

and substituting them in Equation (14.46), the following expression is obtained:

$$-TF(\omega i) = -\frac{\omega^2 e^{-\tau\omega i}}{c_a\omega i + k_a}\Delta g + \frac{\omega^3 i g e^{-\tau\omega i}}{c_a\omega i + k_a}\Delta\tau \tag{14.50}$$

In this equation, g and τ are known from the current control situation, and ω is detected from the zero-crossings of the $\ddot{x}_a$ signal. Though c_a and k_a are unknown, their nominal values are used

(per the above discussion), and $TF(\omega i)$ is known from the complex convolution result (Renzulli 1996; Renzulli et al. 1999). The only unknowns in Equation (14.50) are Δg and $\Delta\tau$, which are solved from two algebraic equations that arise from the complex linear Equation (14.50):

$$\Delta g = \mathrm{Re}\left[TF(\omega i)\frac{c_a \omega i + k_a}{\omega^2 e^{-\tau\omega i}} \right] \tag{14.51}$$

$$\Delta\tau = -\frac{1}{g\omega}\,\mathrm{Im}\left[TF(\omega i)\frac{c_a \omega i + k_a}{\omega^2 - \tau\omega i} \right] \tag{14.52}$$

These are the increments necessary for reducing $|TF(\omega i)| = |TF(\omega i)_{old} + \Delta TF(\omega i)|$, i.e., for improving the DR absorption performance. In the next control step, $(g+\Delta g)$ and $(\tau+\Delta\tau)$ are used in place of g and τ, and the process described in Equations (14.44) to (14.52) is repeated. This leads to further reduction of $|TF(\omega i)|$ as the robust tuning evolves. The process is stopped when $|TF(\omega i)|$ falls within a desirably small value. The convergence of this process is assured if the assumptions regarding C^{∞} and the structural variation speeds hold.

Notice that this strategy requires nothing more than the two acceleration signals, i.e., acceleration of the mass and of the base of the DR. Therefore, the DR vibration absorption scheme remains free-standing. That is, the control logic (both for frequency tracking and robust tuning steps) does not require any external measurements, except those within the DR structure.

14.2.2.2 Tuning to Swept-Frequency Disturbance

The automatic tuning procedure is illustrated on vibration control of the flexible beam of Section 14.2.1.6 subject to disturbance with time-varying frequency. The test setup is shown in Figures 14.5a and 14.5b. In this particular case, the experimentally determined nominal absorber parameters are $m_a = 0.177$ kg, $c_a = 81.8$ kg/s, and $k_a = 3.49 \times 10^6$ N/m. The disturbance frequency is varied between 650 and 750 Hz at a constant rate, maintaining the amplitude fixed. The tests are carried out with sweep rates of 2.4 Hz/s and 10 Hz/s. It is logical to expect that the suppression for the swept-frequency disturbance is worse than in the fixed frequency case of Section 14.2.1.6. When the frequency sweeps, it changes before the DR attains the steady state, necessitating new values of gain and delay for perfect absorption. This settling delay of DR has a computational part (which is due to the iterations of DR autotuning) and an inertial part (due to the dynamic transients of the combined system). Therefore, it is natural that the tuning algorithm will always lag behind. Consequently, the higher the sweep rate, the worse the performance. The results of the two swept-frequency tests are shown in Figure 14.9 for a passive mode of operation, i.e., with the control feedback disconnected, and for the DR absorber with autotuning. The active vibration suppression level is 16 dB minimum for the 10 Hz/s sweep, and 32 dB minimum for the 2.4 Hz/s sweep.

14.2.3 The Centrifugal Delayed Resonator Torsional Vibration Absorber

The centrifugal delayed resonator (CDR) represents a synthesis of the delayed-feedback control strategy and a passive centrifugal pendulum absorber for vibration control of rotating mechanical structures (Hosek 1997; Hosek et al. 1997a and 1999b). The centrifugal pendulum absorber (Carter, 1929; Den Hartog, 1938; Wilson, 1968; Thomson, 1988) is an auxiliary vibratory arrangement in which the motion of the supplementary mass is controlled by a centrifugal force (Figure 14.10a). Considering its linear range of operation, the natural frequency of the centrifugal pendulum absorber is directly proportional to the angular velocity of the primary structure. Therefore, the absorber is effective when the ratio of the frequency of disturbance and the angular velocity of the primary

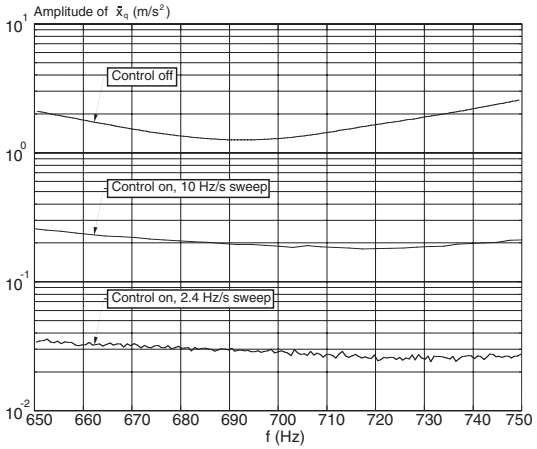

FIGURE 14.9 Beam response to swept-frequency excitation.

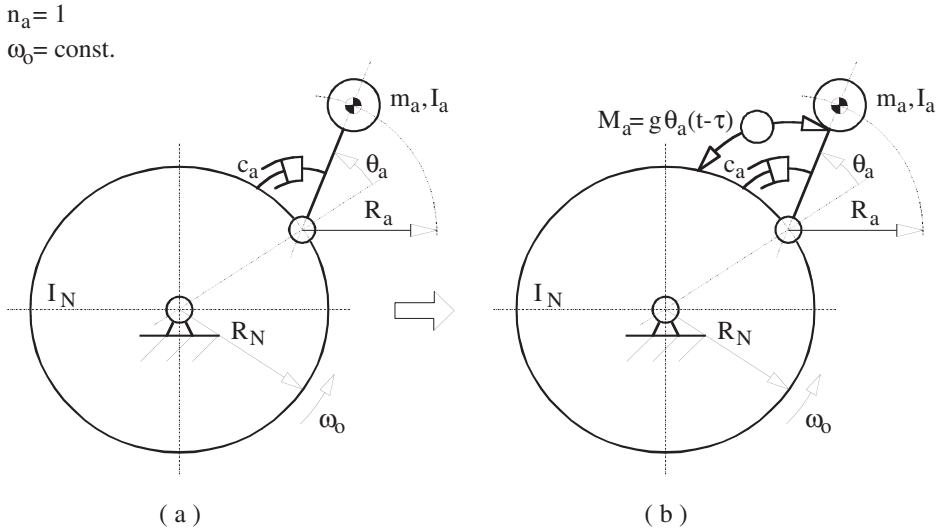

FIGURE 14.10 (a) Damped centrifugal pendulum, (b) centrifugal delayed resonator.

structure remains constant. This is the case in many applications. For instance, the fundamental frequency of the combustion-induced torques acting on the crankshaft in an internal combustion engine is a fixed multiple of the rotational velocity of the crankshaft.

In order to relax the constraint of a constant ratio of the frequency of disturbance and the angular velocity of the primary structure and/or to improve robustness against wear and tear, the CDR vibration suppression technique can be utilized. Similar to the DR vibration absorber, delayed partial state feedback is introduced to convert a damped centrifugal pendulum into an ideal frequency-tunable dynamic absorber. Introducing the real-time tuning ability feature, the CDR can improve performance of passive centrifugal pendulum absorbers in a variety of vibration problems. Typical examples can be seen in crankshaft and transmission systems of aero, automobile, and marine propulsion engines.

14.2.3.1 Concept of the Centrifugal Delayed Resonator

A damped centrifugal pendulum attached to a rotating carrier is depicted schematically in Figure 14.10a. Considering small displacements θ_a and a constant angular velocity ω_o, the linearized differential equation of motion of the system of Figure 14.10a takes the following form (Hosek et al. 1997a, 1999b):

$$(I_a + m_a R_a^2)\ddot{\theta}_a + c_a\dot{\theta}_a + m_a R_N R_a \omega_0^2 \theta_a = 0 \tag{14.53}$$

The natural frequency, damping ratio and resonant (peaking) frequency of the centrifugal pendulum are found as:

$$\omega_a = \sqrt{\frac{R_N}{R_a + I_a/(m_a R_a)}}\,\omega_0 \tag{14.54}$$

$$\zeta_a = \frac{c_a}{2\omega_0\sqrt{m_a R_N R_a (I_a + m_a R_a^2)}} \tag{14.55}$$

$$\omega_p = \omega_a\sqrt{1-2\zeta_a^2} \approx \omega_a \text{ for light damping} \tag{14.56}$$

Equations (14.54) and (14.56) show that the (undamped) natural or resonant frequency of a lightly damped centrifugal pendulum is *directly proportional* to the rotational velocity ω_0. The proportionality constant $n = \omega_a/\omega_0$ is called the *order of resonance* of the passive centrifugal pendulum.

The proportionality between the natural frequency ω_a and the rotational velocity ω_0 has the following physical interpretation. The centrifugal field provides a restoring torque due to which the pendulum tends to return to a radially stretched position, i.e., it acts as a spring with an equivalent stiffness proportional to ω_0^2. Since the natural frequency ω_a is proportional to the square root of the equivalent spring stiffness, it is proportional to the angular velocity ω_0 as well.

Following the DR control philosophy (Secton 14.2.1), the core idea of the CDR concept is to reconfigure the dynamics of the damped centrifugal pendulum arrangement so that it behaves like an ideal tunable resonator. Departing from the passive arrangement in Figure 14.10a, a control torque M_a between the centrifugal pendulum and its carrier is applied in order to convert the system into a tunable resonator, as shown in Figure 14.10b. For this torque, a proportional position feedback with time delay is proposed, i.e., $M_a = g\theta_a(t-\tau)$. The new system dynamics is described by the linearized differential equation of motion (Hosek et al. 1997a, 1999b):

$$(I_a + m_a R_a^2)\ddot{\theta}_a(t) + c_a\dot{\theta}_a(t) + m_a R_N R_a \omega_0^2 \theta_a(t) + g\theta_a(t-\tau) = 0 \tag{14.57}$$

The corresponding Laplace domain representation leads to the following transcendental characteristic equation:

$$C(s) = (I_a + m_a R_a^2)s^2 + c_a s + m_a R_N R_a \omega_0^2 + ge^{-\tau s} = 0 \tag{14.58}$$

To achieve pure resonance, two dominant roots of the characteristic Equation (14.58) should be placed on the imaginary axis at the desired resonant frequency. This proposition results in the following control parameters:

$$g_c = \sqrt{(c_a\omega_c)^2 + [(I_a + m_a R_a^2)\omega_c^2 - m_a R_N R_a \omega_0^2]^2} \tag{14.59}$$

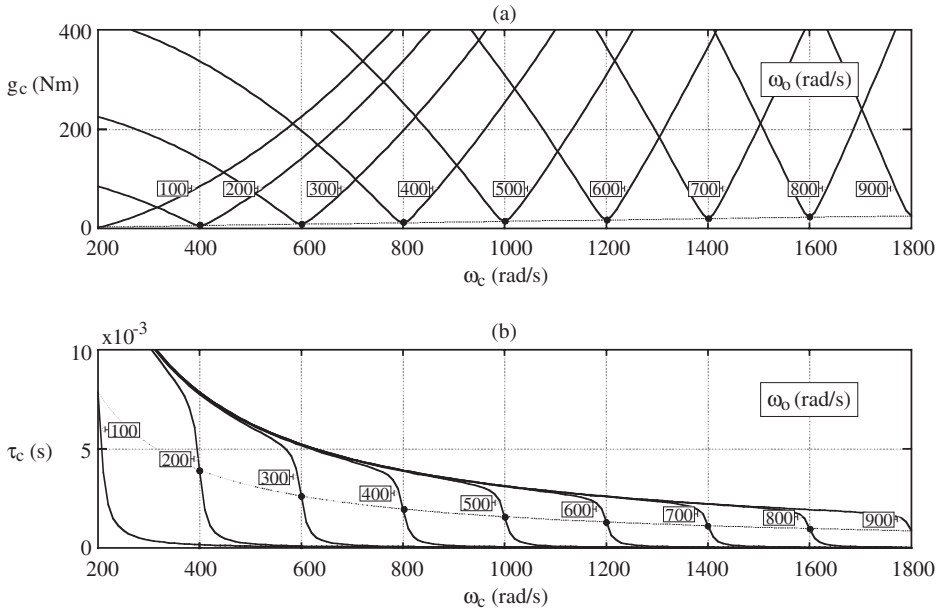

FIGURE 14.11 Feedback gain (a) and delay (b) for the CDR.

$$\tau_c = \frac{\text{atan2}[c_a\omega_c, (I_a + m_a R_a^2)\omega_c^2 - m_a R_N R_a \omega_0^2] + 2(\ell_c - 1)\pi}{\omega_c}, \quad \ell_c = 1,2,3,... \tag{14.60}$$

Similar to j_c in Equation (14.5), the parameter ℓ_c in expression (14.60) indicates the branch of the root loci which is selected to carry the resonant pair of the characteristic roots.

Example plots of the control parameters g_c and τ_c vs. the resonant frequency ω_c, as defined in Equations (14.59) and (14.60), are shown in Figure 14.11. In this particular case, the following parameters are used: $R_N = 0.15$ m, $R_a = 3.749 \times 10^{-2}$ m, $I_a = 2 \times 10^{-7}$ kgm^2, $m_a = 0.5$ kg, $c_a = 2.812 \times 10^{-5}$ kgm^2/s, $\omega_o = 500$ rad/s, and $\tau = 1.571 \times 10^{-3}$ s. The structural parameters R_a, I_a, m_a, and c_a are selected in such a way that the natural frequency (and thus, approximately, the frequency of the resonant peak) of the lightly damped centrifugal pendulum arrangement is twice the angular velocity of the carrier, i.e., $\omega_a = 2\omega_o$, see Equation (14.54). Indeed, the example structure given above possesses this property. The solid curves represent graphs of $g_c(\omega_c)$ and $\tau_c(\omega_c)$ for different values of the angular velocity ω_o in rad/s. The dashed curves correspond to the operating points where the ratio of ω_c and ω_o, i.e., the *order of resonance* for the CDR, remains fixed at $n = 2$.

Figure 14.11 shows that if the frequency ω_c fluctuates around the order of resonance $n = 2$, the CDR always operates near the minimum feedback gain g_c and the maximum sensitivity of the delay τ_c with respect to ω_c. This mode of operation is notable for low energy consumption and excellent tuning ability (Hosek 1997), both of which are desired features when the CDR is used as a tuned vibration absorber.

14.2.3.2 Vibration Control of MDOF Systems Using the CDR

When the CDR is implemented on a rotating multi-degree-of-freedom (MDOF) structure under harmonic torque disturbance, it constitutes an ideal torsional vibration absorber, provided that the control parameters are selected such that the resonant frequency of the CDR and the frequency of the external disturbance coincide.

$n_a = 2$
ω_o = const.

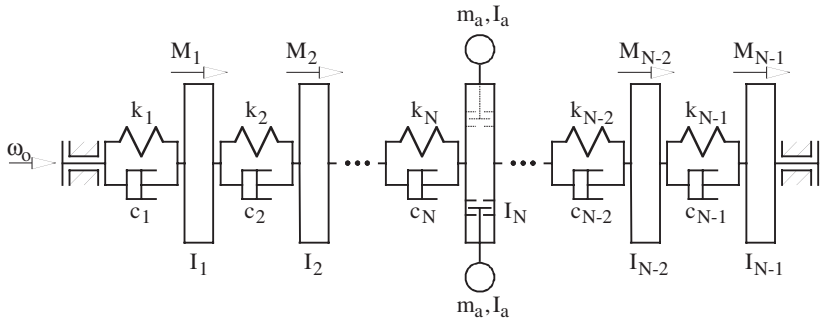

FIGURE 14.12 MDOF structure with the CDR absorber.

The combined system under consideration is depicted in Figure 14.12. A base turning at a constant angular velocity ω_o carries a MDOF primary structure that consists of N lumped disks of inertia moments I_i connected through torsional springs k_i and damping members c_i. The disks are acted on by harmonic disturbance torques $M_i = A_i \sin(\omega t + \varphi_i)$, i = 1, 2, … , N. A CDR absorber is employed at the N-th disk in order to control oscillations resulting from the external disturbance. Although the numbering scheme in this notation is selected so that the CDR is always attached to the disk number N, its implementation on any disk is practically possible, provided that the primary structure is renumbered accordingly.

The dynamic properties of the primary structure alone are represented by a linear differential equation of motion of the conventional form:

$$[I]\{\ddot{\Delta}\} + [C]\{\dot{\Delta}\} + [K]\{\Delta\} = \{M\} \tag{14.61}$$

where [I], [C], and [K] are NxN inertia, damping and stiffness matrices, respectively, $\{M\}$ is an N×1 vector of disturbance torques, and $\{\Delta\}$ represents an N×1 vector of angular differences defined as $\Delta_i = \theta_i - \theta_0$, i = 1, 2, … , N. The linear differential Equation (14.61) is represented in the Laplace domain as:

$$[A(s)]\{\Delta(s)\} = \{M(s)\} \tag{14.62}$$

where:

$$[A(s)] = [M]s^2 + [C]s + [K] \tag{14.63}$$

Considering small angular displacements of the centrifugal pendulum, Equation (14.63) can be expanded for the combined system of the primary structure with the CDR absorber as (Hosek et al. 1999b):

$$\left[\tilde{A}(s)\right]\left\{\tilde{\Delta}(s)\right\} = \left\{\tilde{M}(s)\right\} \tag{14.64}$$

where the matrix $[\tilde{A}(s)]$, augmented vectors of angular differences $\{\tilde{\Delta}(s)\}$ and disturbing torques $\{\tilde{M}(s)\}$ are defined as follows:

$$\tilde{A}_{i,j} = A_{i,j},\ i,j = 1,2,...,N \ \ except \ \ i = j = N \tag{14.65}$$

$$\tilde{A}_{i,N+1} = 0, \quad i = 1,2,...N-1 \tag{14.66}$$

$$\tilde{A}_{N+1,j} = 0, \ \ j = 1,2,...,N-1 \tag{14.67}$$

$$\tilde{A}_{N,N} = A_{N,N} + n_a[I_a + m_a(R_a + R_N)^2]s^2 \tag{14.68}$$

$$\tilde{A}_{N,N+1} = n_a[(I_a + m_a R_a^2 + m_a R_a R_N)s^2 - c_a s - ge^{-\tau s}] \tag{14.69}$$

$$\tilde{A}_{N+1,N} = I_a + m_a(R_a^2 + R_a R_N)s^2 \tag{14.70}$$

$$\tilde{A}_{N+1,N+1} = (I_a + m_a R_a^2)s^2 + c_a s + m_a R_a R_N \omega_0^2 + ge^{-\tau s} \tag{14.71}$$

$$\tilde{M}_i = M_i, \ \ i = 1,2,...,N \tag{14.72}$$

$$\tilde{M}_{N+1} = 0 \tag{14.73}$$

$$\tilde{\Delta}_i = \Delta_i, \ \ i = 1,2,...,N \tag{14.74}$$

$$\tilde{\Delta}_{N+1} = \theta_a \tag{14.75}$$

Applying Cramer's rule, Equation (14.64) is solved for the angular displacement of the *N*-th disk of the primary structure, i.e., the disk to which the CDR is attached:

$$\Delta_N(s) = \frac{[(I_a + m_a R_a^2)s^2 + c_a s + m_a R_a R_N \omega_0^2 + ge^{-\tau s}]\det[Q(s)]}{\det\left[\tilde{A}(s)\right]} = \frac{C(s)\det[Q(s)]}{\det\left[\tilde{A}(s)\right]} \tag{14.76}$$

where:

$$Q_{i,j} = \tilde{A}_{i,j} = A_{i,j}, \ \ i = 1,2,...,N, \quad j = 1,2,...,N-1 \tag{14.77}$$

$$Q_{i,N} = \tilde{M}_i = M_i, \quad i = 1,2,...,N \tag{14.78}$$

Similar to the conventional DR absorber (Section 14.2.1), the factor C(s) in the numerator is found to be identical to the left-hand side of Equation (14.58). Therefore, as long as the denominator possesses stable roots and the CDR is tuned to the frequency of disturbance, i.e., $\omega = \omega_c$, $g = g_c$, $\tau = \tau_c$, the expression $\Delta_N(\omega i)$ is zero and the *N*-th disk of the primary structure exhibits no oscillatory motion in the steady state:

$$\lim_{t \to \infty} \Delta_N(t) = 0 \tag{14.79}$$

In summary, for the frequency of disturbance ω which agrees with the resonant frequency ω_c, the disk of the CDR attachment is quieted completely.

14.2.3.3 Stability of the Combined System

Similarly, to the conventional DR (Section 14.2.1), the range of frequencies of operation of the CDR absorber is restricted due to limitations which arise from stability related issues. Considering small angular displacements, the stability chart method of Section 14.2.1.3 can be used to assess stability of the combined system at a given angular velocity ω_o. Repeating the same stability analysis for angular velocity ω_o varying in a given range of interest, a set of stability limits can be obtained and built into the control algorithm to assure operation of the CDR in the stable zone (Hosek et al. 1997a).

In contrast to the conventional DR, two variables influence stability of the CDR absorber: the angular velocity ω_o and the frequency of disturbance ω. Any change in the angular velocity ω_o has direct influence on the stability properties of the combined system. In reality, however, the changes are smooth and relatively slow due to the inertias involved in the rotating structure. Since ω_o is monitored continuously for the CDR tuning, the stability limits can be updated periodically based on these measurements. The frequency of disturbance, on the other hand, is a property of the external disturbance. Therefore, it has no influence on the system stability until the control parameters g_c and τ_c are modified to correspond to the detected value of ω. Naturally, the controller should implement these modifications only if stable operation is expected, otherwise a passive mode is introduced by setting $g = 0$. Preferably, the stability analysis can be utilized to design the CDR absorber with desirably relaxed stability limitations so that the expected frequencies of disturbance fall into the stable zone.

Since the natural frequency of the centrifugal pendulum arrangement varies with the angular velocity of the primary structure, the overall range of operating frequencies is wider than that of the conventional DR absorber. However, full frequency range is not available at all rotational speeds (Hosek et al. 1997a).

14.2.3.4 Example Implementation

The concept of the CDR is illustrated by a simple prototype absorber. A photograph of the test structure is provided in Figure 14.13a, and a side view of the mechanical design is shown in Figure 14.13b. The main supporting component of the structure is a steel space frame (1). The primary system is represented by an aluminum disk (2) mounted on the shaft of an electric motor (3). The motor (3) is equipped with an integral tachometer to monitor the angular velocity of the shaft. The CDR absorber arrangement comprises the centrifugal pendulum (4), which is coupled pivotably to the disk (2) through an electric motor (5). A linear variable differential transformer (LVDT) (6) is mounted on the disk (2) to measure the relative displacements of the centrifugal pendulum (4). A rotating connector (7) is used to transmit control power for the electric motor (5) and to route low level signals associated with operation of the LVDT (6).

The control system for the test prototype performs two major tasks: nominal velocity control of the primary structure and delayed feedback control of the CDR absorber. The objective of the nominal velocity control is to track a desired overall profile of the angular velocity of the primary structure. This task corresponds, e.g., to a cruise control in an automobile engine application. The CDR control, on the other hand, eliminates undesired oscillations of the primary structure around its nominal velocity. These oscillations can originate, e.g., from periodic forces acting on pistons of an automobile engine. A simple harmonic signal generator is incorporated into the control system to emulate such an external disturbance.

As an example, a harmonic disturbance torque at the frequency of 12 Hz is applied to the primary structure while its nominal angular velocity is kept around 200 rpm. The degree of vibration suppression is visualized in the discrete Fourier transformation (DFT) of the steady-state response, as depicted in Figure 14.14. The scale on the vertical axis is normalized with respect to the maximum magnitude of $\Omega_1(\omega i)$, i.e., the ratio of $|\Omega_1(\omega i)| / \max|\Omega_1(\omega i)|$ is shown in the figure. The light line represents the DFT of the steady-state response of the primary structure with the control feedback disconnected. The bold line depicts the DFT when the CDR control is active. It is observed that the oscillations of the primary structure are reduced by 96%.

FIGURE 14.13a Experimental set-up of CDR.

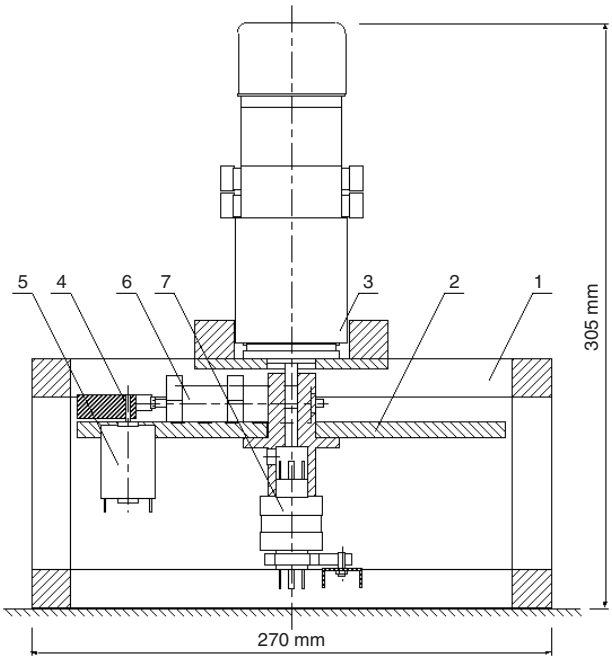

FIGURE 14.13b Side view of CDR test prototype.

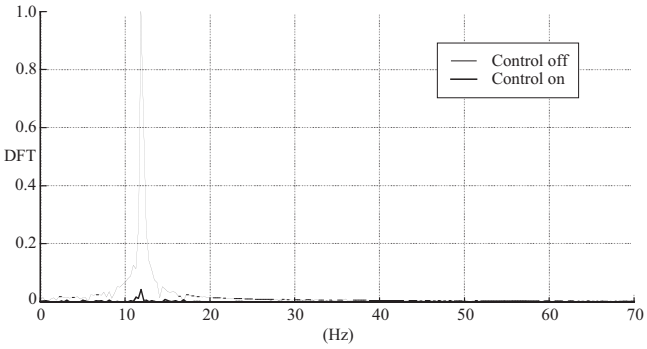

FIGURE 14.14 DFT of the steady-state response of the primary structure to a harmonic disturbance of 12 Hz at a nominal rotational velocity of 200 rpm.

14.2.3.5 Summary

The centrifugal delayed resonator (CDR) is a real-time tunable device for active suppression of torsional vibrations in rotating mechanical structures. It can be viewed as a fine tuning strategy beyond a passive centrifugal pendulum absorber. The preferred frequencies of operation are around the natural frequency of the passive centrifugal pendulum, which is *directly proportional* to the nominal angular velocity of the primary structure. In this mode of operation the CDR consumes relatively low energy and it is easy to tune. This is particularly favorable in applications where the frequency of disturbance is velocity dependent, such as in internal combustion engines, and it constitutes a key contribution of the CDR technique beyond the conventional DR (14.2.1). Similarly, to the conventional DR absorber, the frequency of disturbance can be detected by observing the displacements of the absorber relative to its carrier. Since the feedback gain and delay are functions of the absorber structural parameters and the angular velocity of the rotating base only, see Equations (14.59) and (14.60), the CDR control scheme is *entirely decoupled* from the mechanical and dynamic properties of the primary structure.

14.3 Multiple Frequency ATVA and Its Stability

14.3.1 Synopsis

The actively tuned vibration absorber contains a control, which sensitizes it at multiple frequencies. The feedback law to achieve this can be selected in variety of ways (full state feedback, linear quadratic regulator (LQR) etc.) Here we follow the unconventional feedback structure of Section 14.2. We adopt, however, a position feedback slightly differently, using multiple and unrelated time delays. This control sensitizes the absorber at a number of time-varying frequencies concurrently. It converts the absorber into a multi-frequency resonator (so-called multiple frequency delayed resonator or MFDR). The resonator, in turn, acts as a perfect absorber of vibration at these tuning frequencies when it is attached to a harmonically excited primary system.

The tuning scheme offers the same practical benefits as mentioned earlier (such as simplicity, on-line tuning ability, decoupled nature of the control from the primary). The emphasis of this section, however, is on the stability analysis of such systems with *multiple, unrelated time delays*. Such dynamics and its stability assessment are rarely treated in the literature (Thowsend, 1981b; Marshall, 1979). Thus the problem becomes mathematically very challenging.

An absorber is a dynamic structure, which offers minimum impedance between the excitation force on the primary system and the absorber mass (Sun et al., 1995). This yields relatively high amplitude of oscillations at the absorber for the excitation frequencies of concern (Figure 14.15).

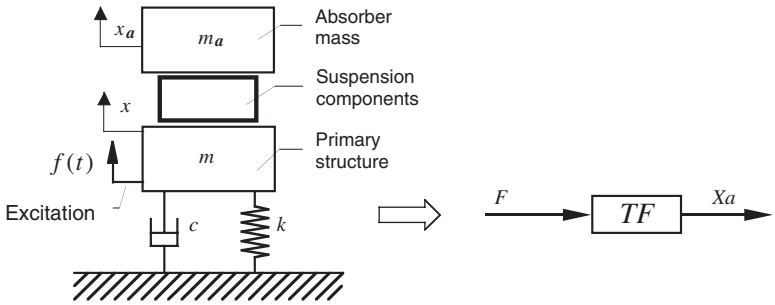

FIGURE 14.15 Typical vibration absorber set-up.

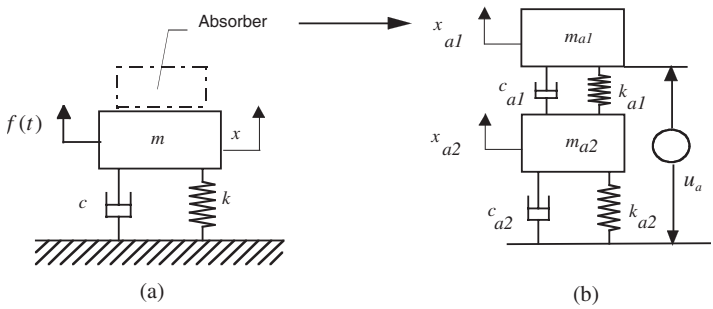

FIGURE 14.16 Primary (a) and absorber (b) structures.

The transfer function x_a/f (inverse of the impedance) should exhibit frequency response characteristics with maxima at the tuning frequencies. The aim in tuning (or 'sensitizing') is to match these frequencies with the dominant frequency contents of f. If this sensitization were assured, the amplitude x_a would be large, implying high energy flow into the absorber.

The most effective absorber is achieved by creating "a resonator," as discussed earlier, at the frequency of the excitation (Olgac et al., 1994; Olgac, 1995; Valášek, 1999). For this, the dominant poles of the absorber substructure are placed on the imaginary axis. Many researchers achieved this objective utilizing various feedback control laws from LQR (linear quadratic regulator) (Seto et al., 1991) to H_∞ (Nishimura et al., 1993) and even neural networks (DiDomenico, 1994) and the DR procedure as described earlier. Here we will expand on the latter concept, which contains a proportional position feedback with a time delay.

The theme of this section is to sensitize the absorber at multiple frequencies. Without loss of generality, we take the case of dual-frequency vibration absorption into account, although the treatment is expandable to general multiple frequency cases. The dynamic model is analyzed from the perspective of transmissibility; along with the stability of the controlled structure.

Consider the primary structure in Figure 14.16 which is subjected to time varying dual frequency excitation:

$$f(t) = f_1 \sin \omega_1 t + f_2 \sin \omega_2 t\,. \tag{14.80}$$

where ω_1 and ω_2 vary in steps as time progresses. In order to suppress undesired oscillations of the primary mass, m, a lightly damped passive absorber is suggested. Ideally, it should have two pairs of poles at $\pm i\omega_1$ and $\pm i\omega_2$. Even a small damping (i.e., c_{a1}, c_{a2}) could remove the poles from these ideal settings. Consequently, the vibration caused by the dual harmonic forcing will not be

fully suppressed. A plausible two DOF absorber structure to achieve this is given in Figure 14.16b. Fine-tuning of the absorber poles requires a feedback control, which aims to

1. Make the absorber resonant at ω_1 and ω_2 by enforcing the absorber poles at $\pm i\omega_1$ and $\pm i\omega_2$. This pole placement operation is indeed the tuning of the absorber (i.e., to place the poles of the absorber structure at ω_1 and ω_2 precisely) so that the absorption is perfected at these frequencies. This process can also be considered as equivalent to eliminating the damping component at these poles.
2. Achieve tuning for time varying frequencies.

Typically, the excitation frequencies ω_1 and ω_2 are assumed to vary within a narrow range around the passive absorber's natural frequencies. Otherwise the above described pole placement procedure requires a large control authority, which is often not practicable.

Considering the system depicted in Figure 14.16, the governing equations are written as follows:

for the absorber alone (Figure 14.16b),

$$\begin{aligned} &m_{a1}\ddot{x}_{a1} + c_{a1}(\dot{x}_{a1} - \dot{x}_{a2}) + k_{a1}(x_{a1} - x_{a2}) + u_a = 0, \\ &m_{a2}\ddot{x}_{a2} + c_{a2}\dot{x}_{a2} + k_{a2}x_{a2} - c_{a1}(\dot{x}_{a1} - \dot{x}_{a2}) - k_{a1}(x_{a1} - x_{a2}) = 0; \end{aligned} \tag{14.81}$$

and for the combined system (primary structure and the absorber together),

$$\begin{aligned} &m_{a1}\ddot{x}_{a1} + c_{a1}(\dot{x}_{a1} - \dot{x}_{a2}) + k_{a1}(x_{a1} - x_{a2}) + u_a = 0, \\ &m_{a2}\ddot{x}_{a2} + c_{a2}(\dot{x}_{a2} - \dot{x}) + k_{a2}(x_{a2} - x) - c_{a1}(\dot{x}_{a1} - \dot{x}_{a2}) - k_{a1}(x_{a1} - x_{a2}) = 0, \\ &m\ddot{x} + c\dot{x} + kx - c_{a2}(\dot{x}_{a2} - \dot{x}) - k_{a2}(x_{a2} - x) - u_a = 0. \end{aligned} \tag{14.82}$$

Notice that the control feedback force, u_a, is implemented between the base of the absorber and the mass m_{a1}. This is a design choice that is not unique and does not affect the generalization of the work presented here.

Extending an earlier proposition (Valášek et al., 1999) the control for the above pole placement is chosen in the form of superimposed delayed position feedback:

$$u_a = \sum_{i=1}^{4} g_i(x_{a1}(t - \tau_i) - x(t - \tau_i)) \tag{14.83}$$

This is identical to having four retarded springs with stiffness g_i and retardation τ_i between the absorber mass m_{a1} and the absorber base. τ_i delays are preselected and the gains are periodically updated for tuning, as explained below. An important point to note is the nature of the feedback control. It is formed by the delayed relative displacements between the absorber and the primary structure. Therefore, the process is decoupled from the primary side. That is, the absorber can be tuned independently from the dynamic features of the primary structure, i.e., its mass, stiffness etc.

Laplace domain representation of Equations (14.81 and 14.82) is

for the **absorber**

$$\begin{bmatrix} m_{a1}s^2 + c_{a1}s + k_{a1} + \sum_{i=1}^{4} g_i e^{-\tau_i s} & -c_{a1}s - k_{a1} \\ -c_{a1}s - k_{a1} & m_{a2}s^2 + (c_{a2} + c_{a1})s + (k_{a2} + k_{a1}) \end{bmatrix} \cdot \begin{bmatrix} X_{a1} \\ X_{a2} \end{bmatrix} = \mathbf{A}_{\mathbf{abs}} \cdot \begin{bmatrix} X_{a1} \\ X_{a2} \end{bmatrix} = \mathbf{0} \tag{14.84}$$

and for the **combined system**

$$\begin{bmatrix} m_{a1}s^2 + c_{a1}s + k_{a1} + \sum_{i=1}^{4} g_i e^{-\tau_i s} & -c_{a1}s - k_{a1} & -\sum_{i=1}^{4} g_i e^{-\tau_i s} \\ -c_{a1}s - k_{a1} & m_{a2}s^2 + (c_{a2} + c_{a1})s + (k_{a2} + k_{a1}) & -c_{a2}s - k_{a2} \\ -\sum_{i=1}^{4} g_i e^{-\tau_i s} & -c_{a2}s - k_{a2} & ms^2 + (c + c_{a2})s + (k + k_{a2}) + \sum_{i=1}^{4} g_i e^{-\tau_i s} \end{bmatrix} \cdot \begin{bmatrix} X_{a1} \\ X_{a2} \\ X \end{bmatrix} = \mathbf{A}_{\mathbf{cs}} \cdot \begin{bmatrix} X_{a1} \\ X_{a2} \\ X \end{bmatrix} = \mathbf{0} \qquad (14.85)$$

In these equations capital letters correspond to the Laplace transformed quantities of the respective lower case expressions; $\mathbf{A}_{\mathbf{cs}}$ is the system matrix for the combined system and $\mathbf{A}_{\mathbf{abs}}$ is that of the absorber.

The objective is to make this absorber resonant at two distinct frequencies at the same time. This tuned absorber is named dual frequency delayed resonator (DFDR). The two pairs of characteristic roots of the absorber substructure are placed at $\mp\omega_1 i$ and $\mp\omega_2 i$, by imposing these as roots to the respective characteristic equations:

$$CE_{abs} = \det \mathbf{A}_{\mathbf{abs}}\big|_{s=\omega i} = 0 \qquad \omega = \omega_1 \text{ and } \omega = \omega_2 \qquad (14.86)$$

Equation (14.86) is complex-valued and forms a set of four simultaneous linear equations in g_i's:

$$\begin{aligned} &\mathrm{Re}[CE_{\mathbf{abs}}] = 0 \text{ for } s = \omega_1 i \text{ and } s = \omega_2 i \\ &\mathrm{Im}[CE_{\mathbf{abs}}] = 0 \text{ for } s = \omega_1 i \text{ and } s = \omega_2 i \end{aligned} \qquad (14.87)$$

which can be solved readily. The solutions $\bar{g} = \{g_i\}$ and the selected τ_is are the feedback parameters. Notice that Equation (14.86) is transcendental, thus it invites many other finite roots as well as the four of interest. Desirably, but not necessarily, these additional roots should be in the stable left half plane. The stability of the combined system, therefore, needs to be studied for the effective suppression of vibration. Interestingly the stability of the absorber subsection is not required as long as the combined system is guaranteed to be stable. Details of this argument can be found in (Olgac et al., 1997) for single frequency DR cases.

When the absorber is tuned, the transfer function between the primary and absorber masses should exhibit an impedance picture with two zeros, such as Figure 4.17. In this figure $|x/x_a|$ refers to the frequency ratio of the two amplitudes, i.e., $|x(s=\omega i)/x_a(s=\omega i)|$. In order to suppress the oscillation of the primary at a given frequency, $|x/x_a|_{s=\omega i}$ should be very close to zero. This ratio, indeed, is the ratio of the two respective impedances, i.e., the impedance at the primary side, F/x, should be large, while

$$\frac{F/x_a}{F/x} = \frac{\text{impedance for } F \rightarrow x_a \text{ transition}}{\text{impedance for } F \rightarrow x \text{ transition}}$$

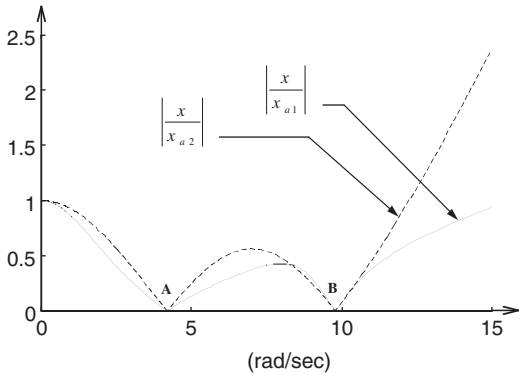

FIGURE 14.17 Primary/absorber amplitude ratios for a typical case of tuned absorber with dual resonance frequencies (at A and B).

is comparatively much smaller. This implies that the primary substructure passes the vibratory energy in full to the absorber section at the particular frequency of resonance. This is the core phenomenon yielding the absorber sensitization and effective vibration absorption.

Obviously, the absorber is sensitized to suppress oscillations at the two frequencies ω_1 and ω_2. This sensitization can be readjusted in real time for a different set of frequencies. The process requires simply recalculating the g_i's as described earlier. The two frequencies, ω_1 and ω_2, need to be detected as they vary in time. One way of achieving this is to check the time traces of the absorber motion and extract its frequency contents. This calls for a "shifting window" type FFT, and it is also possible to do in real-time (Orfanidis, 1996). In order to allow the system, however, to complete the transient regime prior to the adjustment in $\{g_i\}$, this process is repeated at a slower pace than the settling period of the combined system.

An outstanding operational issue in this active vibration suppression process is the on-line assessment of the stability. Notice that the system at hand (Equations 14.84 and 14.85) has transcendental characteristic equations with four unrelated time delays. There is very limited knowledge available in the dynamic systems literature on such systems containing unrelated delays (Huang and Olgac, 2000; Stepan, 1989). An interesting treatment can be found in (Hertz et al., 1984) for commensurate delays, i.e., delays that are integer multiples of a core delay. Recently, a systematic methodology was suggested by the group of the authors (Huang and Olgac, 2000) to address this issue. The method forms the highlight of the present work. Before going into the stability analysis we wish to touch upon the selection of τ_i's. A rudimentary selection method is used for the time delays τ_i. We take a relatively even distribution of $\{\tau_i\}$, such that even the largest τ_i would not cause aliasing in the feedback. That is, the largest time delay is much less than the smallest period of the excitation on hand. The case study example follows this logic.

14.3.1.2 Stability Analysis; Directional Stability Chart Method

The combined system as given in Equation (14.85), should be asymptotically stable. Notice that in this equation, only ω_i's (excitation frequencies) are the variables yielding the values of $\{g_i\}$ and in turn the stability of the operation. For an arbitrary set of (ω_1, ω_2), and the corresponding $\{g_i\}$ the characteristic equation

$$CE_{cs} = \det \mathbf{A}_{cs} = 0 \tag{14.88}$$

is either stable, marginally stable, or unstable. It has a general form of

$$CE_{cs}[\bar{g}, \bar{\tau}, s] = 0 \tag{14.89}$$

where $\bar{\tau}$ is the preselected time delay vector with the components of τ_i, and $\bar{g} = \{g_i\}$. It is clear that for $\bar{g} = 0$ the system represents the passive structure, and it is inherently stable. From this point we follow a recently introduced stability assessment strategy which is called the directional stability chart method (DSCM) (Huang and Olgac, 2000) in the structured steps given below:

1. Substitute $\{g_i\}$ with $\{\lambda g_i\}$, where $\lambda \in [0,1]$ is the interpolation constant.
2. Suppressing the known terms in the argument the reduced form of Equation (14.88) becomes

$$CE_{cs}[\lambda, s] = 0 \tag{14.90}$$

3. Substitute $s = i\omega$ and find the values of $\lambda \in [0,1]$ which yield imaginary roots to Equation (14.90). That is, we solve λ and ω from the complex valued equation

$$CE_{cs}[\lambda, \omega] = 0 \tag{14.91}$$

which yields two real equations for the unknowns $\lambda \in [0,1]$ and $\omega \in [0, \omega_{high}]$. These two simultaneous nonlinear equations can be solved using commercial packages (such as MATLAB or MAPLE). Here ω_{high} is an upper bound for the root finding routine beyond which such an imaginary root does not exist. This value is case specific and can be determined mathematically or observed graphically.
Let's assume m such solution pairs (λ_i, ω_i), i = 1…m are found for which there is a pair of characteristic roots on the imaginary axis.
4. Determine the root sensitivities at each of these root crossing points with respect to λ by differentiating Equation 14.88 and using the imaginary root corresponding to this λ_i, i.e., s = ω_i i. That is,

$$\frac{\partial}{\partial s} CE_{cs}(\lambda, s)\ ds + \frac{\partial}{\partial \lambda} CE_{cs}(\lambda, s)\ d\lambda = 0 \tag{14.92}$$

The root sensitivity is defined as:

$$S_s^{\lambda} = \frac{ds}{d\lambda}\Big|_{\lambda_i, \varpi_i} \tag{14.93}$$

If the real part of the root sensitivity, Re (S_s^{λ}), is positive then increasing λ_i at that point would give rise to two new unstable poles. On the contrary, if the root sensitivity is negative, then increasing λ_i would decrease the number of unstable poles by two, implying the two unstable poles migrate to stable zone.
5. Scan the m solutions of (4) from the smallest to the largest value of $\lambda \in [0,1]$ and create a table of stability outlook which shows the number of unstable roots at each interval of λ. Note that the starting point λ= 0 (i.e., no feedback control) for most physical systems (certainly for the one chosen in Figure 14.16) is asymptotically stable, i.e., no unstable right half roots exists.
6. The last interval $\lambda_m < \lambda < 1$ dictates the stability properties of the system in Equation (14.83) which corresponds to λ= 1. Notice that, λ= 1 implies that the full values of the gains $\{g_i\}$ are used as determined from Equation (14.87).
7. If λ= 1 represents stable operation, we further continue for $\lambda > 1$ until such λ_c is reached that yields marginal stability. The value of λ_c indicates the proximity of the operating point to the marginal stability. The larger the λ_c the better the stability.

The systematic steps of (1–7) represent a D-subdivision method (Kolmanovskii and Nosov, 1986) application in one dimension (λ). The method states that as parameter λ varies from 0 to 1 the number of unstable roots changes only at the points of (λ_i, ω_i), i = 1…m and the change is in the direction indicated by step (4). As this search is performed along the vector direction of $\{g_i\}$ the new methodology is called the directional stability chart method (DSCM).

DSCM procedure enables the user to assess the stability of the absorber at a given set of (ω_1, ω_2). This method can be used to establish operable (i.e., stable) vs. inoperable (i.e., unstable) sectioning in the (ω_1, ω_2) plane. These sections are determined off-line (a priori to the controls). In real-time applications the controller should first detect the present excitation frequencies (ω_1, ω_2), then check whether this point falls in the operable or inoperable zone, and ultimately activate the tuning control if the point (ω_1, ω_2) is in the operable zone.

14.3.1.3 Example Case

As a case study, an absorber with two masses is taken into account (as shown in Figure 14.16b), which is attached to an SDOF primary structure. The numerical values used for the simulations are:

$$m = 50 \text{ kg}; \quad c = 49.6 \text{ kg/s}; \quad k = 1922 \text{ N/m};$$
$$m_{a1} = 1 \text{ kg}; \quad c_{a1} = 1.32 \text{ kg/s}; \quad k_{a1} = 30.25 \text{ N/m};$$
$$m_{a2} = 1 \text{ kg}; \quad c_{a2} = 0.39 \text{ kg/s}; \quad k_{a2} = 42.25 \text{ N/m};$$

The feedback structure of Equation (14.83) is used with $\tau_1 = 0.05$ sec, $\tau_2 = 0.1$ sec, $\tau_3 = 0.2$ sec, and $\tau_4 = 0.25$ sec delays. As described earlier the gains are calculated for the resonance frequencies: $\overline{\omega} = [\omega_1, \omega_2] = [4.2,\ 9.8]$ rad/sec, as:

$$g_0 = \begin{bmatrix} g_1 \\ g_2 \\ g_3 \\ g_4 \end{bmatrix} = \begin{bmatrix} -389.8606 \\ 667.5552 \\ -418.0914 \\ 194.7341 \end{bmatrix} \text{ (N/m)}$$

Notice that the τ_i's are evenly distributed between 0 and 0.25 sec. This maximum time delay is selected such that the aliasing will not appear even for the system response to 4.2 rad/sec excitation.

For this set of (ω_1, ω_2) we proceed with the directional stability chart method (DSCM) to check if Equation (14.91) has a solution in the interval of $\lambda \in [0,1]$. If it does not the combined system *together with the tuned absorber* is stable. As explained in Section 14.3.1.2(f) the range of the search is extended beyond $\lambda \in [0,1]$. The first root encountered is

$$\lambda_c = 1.0428; \quad \omega_{crossing} = 9.6648 \text{ rad/s};$$

and the corresponding $\text{Re}[ds/d\lambda] = 1.2178 > 0$ implying the passage of two stable roots to the right hand unstable plane. Notice the directional stability margin, the value of λ_c is only 4% larger than 1. That means keeping everything else fixed if we increase the operating gains $\overline{g}_0$ by 4% the combined system would become resonant (i.e., marginally stable).

Figure 14.18 shows the primary mass response $x(t)$, as well as the absorber displacements, $x_{a1}(t)$ and $x_{a2}(t)$ shown as insets when the primary structure experiences a dual harmonic excitation force

$$f(t) = \sin \omega_1 t + \sin \omega_2 t.$$

The oscillations are suppressed as the absorbers react with large amplitudes. The structure settles in at 50 seconds and then the two excitation frequencies are changed to

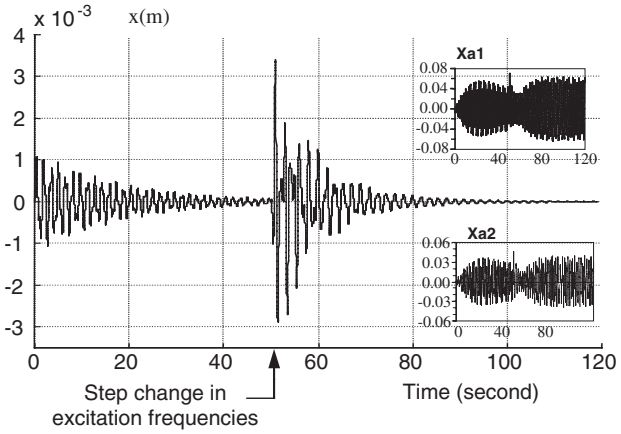

FIGURE 14.18 Time histories of x, x_{a1}, x_{a2} as the excitation frequencies ω_1 and ω_2 vary.

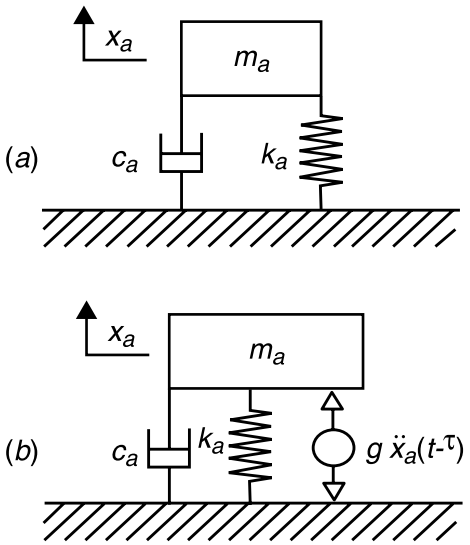

FIGURE 14.19 (a) Passive absorber, (b) delayed absorber with acceleration feedback.

$$\omega = [3.5,\ 9.2]\ \text{rad/sec}$$

by a step function. This sudden variation is observed in Figure 14.18. The absorber section is retuned to these two frequencies by the selection of new gains:

$$\begin{aligned} g_1 &= -494.6554 \\ g_2 &= 808.3025 \\ g_3 &= -514.6770 \\ g_4 &= 185.0157 \end{aligned} \qquad \text{(N/m)}$$

while keeping the delays (τ_is) the same.

We follow the DSCM again for this new pair of (ω_1, ω_2) and show that there is no root for $\lambda \in [0,1]$. Therefore, the system still remains stable (operable). The suppression of the oscillation at the new frequencies, takes effect within about 50 seconds again. Notice, in this time interval the absorbers settle in their steady state response modes. This exercise shows the on-line tuning ability of the absorber section.

One critical issue in the above procedure is the determination of the excitation frequencies imposed on the primary system. It can only be achieved implementing FFT on the absorber displacement with a shifting window. The delay, which is caused by this process, is an issue in our ongoing research. It forces the control gain updates to be as frequent as the availability of the new ω_i's. For the example case above, it was assumed that the new values of ω_i's are instantly available to the controller.

14.3.2 Optimum ATVA for Wide-Band Applications

We next present a summary from an optimization effort reported in (Jalili and Olgac, 2000). The objective here is not a precise tuning of the ATVA to a number of frequencies; a frequency band of suppression is aimed for instead. This feature is achieved through a compromise of imperfect suppression at a given frequency.

14.3.2.1 Synopsis

The active tuning of the absorber is again achieved using partial state feedback with a controlled time delay. The final structure, which is named delayed feedback vibration absorber (DFVA), is optimized to yield minimum M_{peak} of the primary system involved for a given wide band of excitation frequencies. The optimization is performed over the absorber's structural parameters and the features of the feedback control. The assurance of the stability of the time-delayed system, which forms a critical constraint on the optimization, is also considered.

ATVA is typically formed by feedback which places the poles of the absorber section at some desired locations in order to create the spectral effects mentioned earlier (Jalili and Olgac, 2000). For instance, the DR strategy creates two dominant poles on the imaginary axis, but infinitely many finite poles at other locations (due to the time delay). As mentioned earlier, this procedure yields some undesirable M_{peak} at other frequencies. In this work we reiterate the DR feedback formation to place the dominant poles away from the imaginary axis, to an optimum location such that the primary system exhibits $min\{M_{peak}\}$ possible. Notice that the feedback strategy remains as simple as the case in DR, but the new flexibility, the placement of the dominant poles, offers a vehicle for further improvement such as performance optimization.

14.3.2.2 Delayed Feedback Vibration Absorber (DFVA)

A conventional passive absorber (Figure 14.19a) is reconfigured using a delayed *acceleration feedback* (Figure 14.19b). This forms the delayed feedback vibration absorber (DFVA). The corresponding new system dynamics and the respective characteristic equation are

$$m_a \ddot{x}_a(t) + c_a \dot{x}_a(t) + k_a x_a(t) - g\ddot{x}_a(t-\tau) = 0 \tag{14.94}$$

$$m_a s^2 + c_a s + k_a - g s^2 e^{-\tau s} = 0 \tag{14.95}$$

By selecting the control parameters g and τ properly, the dominant roots can be moved anywhere off the imaginary axis. This general DFVA lends itself to an optimization process for the most desirable location of these dominant roots. The effort in this work is to re-tune the DR feedback gain, g, and time delay, τ, such that the peak frequency response of the primary structure attains its global minimum, over a desired "*wide band*" frequency range. In the following sections, the

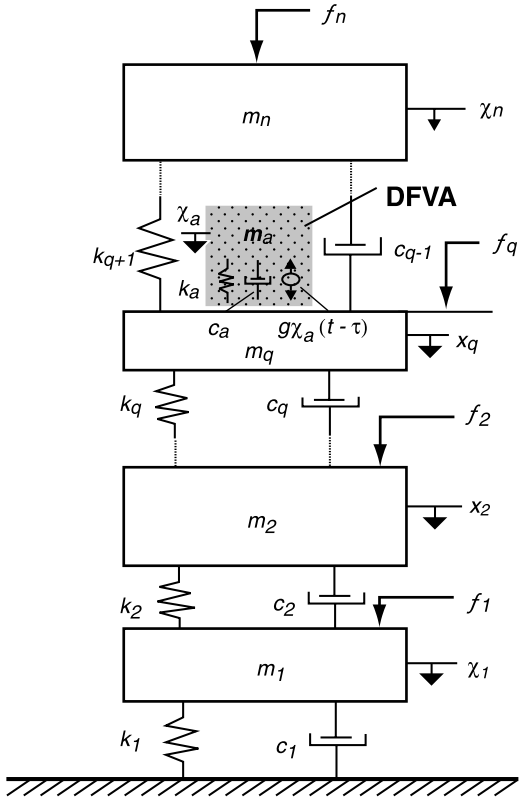

FIGURE 14.20 The DFVA implementation on an n-DOF structure.

governing equations of the dynamics and the selection procedure for the control parameters are presented.

The DR vibration absorber can be considered as a special case of DFVA. For an ideal DR, the dominant poles of the characteristics equation are placed on the imaginary axis $s = \pm j\omega_c$, at a designated frequency ω_c. As stated earlier, the DR offers perfect absorption at this frequency, but to the cost of worsening frequency response at the adjacent frequencies. This can be improved by different formation of feedback such that the dominant poles are positioned away from the imaginary axis, at some optimum locations. In this case, the primary system's frequency response would not be zero anywhere, but it will be flat over a desired frequency range, say $[\omega_{low}, \omega_{up}]$, around a specified center frequency ω_c. The strategy for the control parameters' selection and the end effects are discussed in what follows.

14.3.2.3 The Governing Equations

A general *n* degree-of-freedom (DOF) mechanical system is considered with a DFVA for suppressing undesired oscillations caused by wide band force excitations. The resulting combined system, the DFVA appended on the primary structure, is depicted in Figure 14.20. The DFVA is attached on the *q*-th mass (or DOF) of the primary structure. The objective of this work is twofold: to tune the control parameters g and τ, and to select the passive absorber characteristics m_a, c_a, and k_a, such that the frequency response of the *q*-th mass, on the primary system, is minimized in a given frequency interval.

The state-space representation of this system is written in the form of linear simultaneous differential equations, see (Jalili and Olgac, 2000) for details.

$$\dot{\mathbf{y}}(t) = \mathbf{A}_0 \mathbf{y}(t) + g\, \mathbf{A}_\tau\, \dot{\mathbf{y}}(t-\tau) + \mathbf{f}(t) \qquad t \geq t_0 \tag{14.96}$$

where

$$\mathbf{y}(t) = \{\ \underbrace{x_1, \dot{x}_1, ..., x_n, \dot{x}_n}_{2n}, x_{a1}, \dot{x}_{a1}\ \}^T,\ \mathbf{f}(t) = \{\ \underbrace{0, f_1, ..., 0, f_n}_{2n}, 0, 0\ \}^T \in \Re^{2(n+1)\times 1}$$

are the state variable and excitation vectors. The displacements of the primary structure and the absorber are denoted by $x_i(t)$, $i = 1, 2, ..., n$ and $x_a(t)$, respectively. $\mathbf{A}_0$ and $\mathbf{A}_\tau \in \Re^{2(n+1)\times 2(n+1)}$ are the constant system matrices, τ and g are the time delay and feedback gain.

The Laplace domain representation of the system is

$$(s\mathbf{I} - \mathbf{A}_0 - g\, s\, e^{-\tau s}\mathbf{A}_\tau)\ \mathbf{Y}(s) = \mathbf{F}(s) \ \Rightarrow\ \mathbf{H}(s)\ \mathbf{Y}(s) = \mathbf{F}(s) \tag{14.97}$$

and the corresponding characteristic equation is

$$|\mathbf{H}(s)| = \det[\ s(\mathbf{I} - g\, e^{-\tau s}\, \mathbf{A}_\tau) - \mathbf{A}_0\ ] = 0 \tag{14.98}$$

For each $g \neq 0$ and $\tau \neq 0$, Equation (14.98) has infinite number of roots, which are called the *spectrum* of the time-delayed system.

The Equation (14.97) yields a solution for $x_q(t)$. The objective of the ATVA is to bring $x_q(t)$ to zero or as close to it as possible.

14.3.2.4 Optimum DFVA

As stated before, the objective of this study is to minimize the maximum system response to a wide band excitation. By performing a number of simulations, it is shown that both flattening the frequency response and minimizing the peak frequency yield the same result. In fact, this is analytically proved for the passive absorber attached to an undamped primary structure (Bapat et al., 1979; Warburton et al., 1980). To the best of our knowledge, there is no companion analytical proof in cases where the primary is damped.

The numerical problem encountered here is a min-max problem: to find the absorber parameters m_a, c_a, k_a, g, and τ which minimize the supremum of the frequency response $X_q(\omega)$. As such, we seek the optimal absorber parameters $\mathbf{X}_{abs} = [m_a\ k_a\ c_a\ g\ \tau]^T$ to

$$\min_{\mathbf{X}_{abs}} \left\{ \max_{\omega_{low} \leq \omega \leq \omega_{up}} [X_q(\mathbf{X}_{abs}, \omega)] \right\} \tag{14.99}$$

subject to the physical bounds

$$m_a,\ k_a,\ c_a,\ g, \text{ and } \tau\ >\ 0 \tag{14.100}$$

The numerical procedure for this optimization is discussed in what follows. Notice that the passive absorber, i.e., $g = 0$, is always stable. The stability issue arises when active control is used. Especially, the delay element in the feedback can drive the system to instability. As the control parameters g and τ are used for optimization, their influence on the system stability should be studied in parallel. While the dominant characteristic poles of the absorber are placed at some optimum locations, away from the imaginary axis, the poles of the combined system should remain in the left-half of complex plane.

The stability assurance imposes some limitations on the control parameters g and τ. This introduces an additional constraint to the inequalities (14.100) for the proposed optimization problem, described by Equation (14.99). This problem is treated next.

14.3.2.5 Stability of the Combined System

For a time-delayed system, such as the one described in Section 14.3.2.2, the stability analysis is relatively difficult since the characteristic equation is transcendental rather than algebraic. The stability properties of such a complicated configuration are addressed in some earlier works (Olgac et al. 1997; 1996). The sufficient and necessary condition for asymptotic stability is that the roots of the characteristics Equation (14.98), all have negative real parts. This equation is transcendental and the verification of the root locations is not trivial.

It is typical that increasing feedback gain g causes instability as the roots move from left to right of the complex plane as shown in Olgac and Hosek (1997) and briefly described in Section 14.2.1.3). In summary, Olgac and Hosek (1997) conclude the following: for a given delay τ, the operating gain g should be smaller than the gain for which the global system becomes marginally stable using the same delay, τ. The ratio of these two gains $g_{cs}(\tau)/g(\tau)$ can be defined as the stability margin of the control system, for that delay value τ. The comparison of the parametric plots of $g_{cs}(\omega_{cs})$ vs. $\tau_{cs}(\omega_{cs})$ for the combined system with the $g(\omega_c)$ vs. $\tau(\omega_c)$ of the DFVA reveals this stability picture for a range of τ's. See (Olgac et al. 1997) for details.

14.3.2.6 Optimization Scheme

We seek the optimum absorber characteristics vector $\mathbf{X}_{abs} = [m_a\ k_a\ c_a\ g\ \tau]^T$, such that the peak value of the frequency response amplitude of the q-th mass, as given in Equation (14.99), is minimized. The process would also flatten the frequency response of the system. This proposition forms a min-max problem: we wish to minimize the maximum frequency response over a desired frequency range. The optimization process has to comply with some constraints, as described next.

Following earlier explanations, increasing feedback gain g while time delay τ is kept constant, drives the combined system through the stable, marginally stable, and ultimately to the unstable behavior. For a particular delay $\tau = \tau_0$, the combined system crossings, $\omega_{csl}(\tau_0)$ are determined from Equation (14.97) along with the corresponding gains. Notice that, the multiplicity of the gains appears due to the transcendental nature of the characteristic equation for one fixed time delay. To ensure stability of the system, the feedback gain g should be smaller than the infemum of these g_{csl} (ω_{csl}) values. That is,

$$g < g_{\min}\ (\omega_{csl}\ (\tau)), \tag{14.101}$$

where

$$g_{\min} = \text{infemum}\begin{Bmatrix} g_{cs}(\omega_{cs1}) \\ g_{cs}(\omega_{cs2}) \\ g_{cs}(\omega_{cs3}) \\ \vdots \end{Bmatrix}, \quad \text{for} \quad \tau = \tau_0 \tag{14.102}$$

Thus, the plot of $g_{min}(\omega_{cs})$ vs. $\tau_{cs}(\omega_{cs})$ is the lower envelope of the parameterized stability plot of the combined system, $g_{cs}(\omega_{cs})$ vs. $\tau_{cs}(\omega_{cs})$. This envelope is numerically obtained for each "m_a, c_a, k_a" set of absorber parameters, yielding the constraint in Equation (14.101).

It is assumed that primary system parameters are all kept fixed during the optimization procedure. For the passive absorber, typically the optimized values of the stiffness and damping are between

their physical bounds, whereas the optimum value of the absorber mass is always found at the upper bound (Jacquot, 1978; Esmailzadeh et al., 1998; Ozguven et al., 1986). Thus, we select an absorber mass and keep it fixed for simplicity. The optimization is performed only over the four dimensional vector; the spring stiffness, damping coefficient, feedback gain, and time delay, which defines the absorber and control characteristics, $\mathbf{X}_{\text{abs}} = [k_a\ c_a\ g\ \tau]^{\text{T}}$.

The proposed constrained optimization problem is now recast in the form:

$$J = \underset{\mathbf{X}_{abs}}{Min}\ \left\{\ \underset{\omega_{low}\le\omega\le\omega_{up}}{Max}\ [X_q(\mathbf{X}_{abs},\omega)]\ \right\},\qquad \text{for } \mathbf{X}_{abs} = [\,k_a,\ \ c_a,\ \ g\ \ \tau]^T \tag{14.103}$$

subject to physical bounds

$$\begin{aligned} h_1 &\equiv -k_a < 0,\\ h_2 &\equiv -c_a < 0,\\ h_3 &\equiv -g < 0,\\ h_4 &\equiv -\tau < 0, \end{aligned} \tag{14.104}$$

and the stability constraint

$$h_5 \equiv g - g_{\min} < 0 \tag{14.105}$$

The upper bounds k_a^{up} and c_a^{up} are chosen considering some practical limitations. A set of initial values of $\mathbf{X}_{\text{abs}}$ starts the process. These k_a and c_a parameters are taken from a preliminary study: the optimal passive absorber (obviously for $g = 0$), which is the result of the same optimization problem as in Equation (14.103) except for $g = 0$. The initial g and τ are selected based on the DR which uses the optimal passive absorber and operates at the resonance frequency of the primary structure, ω_{peak}. The optimum value of $\mathbf{X}_{\text{abs}}$ is numerically determined, in such a way that the cost function described in Equation (14.103) subject to constraints, Equations (14.104 and 14.105), is minimized.

It should be noted that the stability constraint, expression Equation (14.105), changes simultaneously in each iteration. This is due to the dependence of this constraint on the absorber spring stiffness, k_a, and damping coefficient, c_a, which happen to be a part of the parameter vector sought.

Since the computation of the higher derivatives of the objective function $G(\mathbf{X}_{\text{abs}})$ is very complicated, we deploy optimization techniques which use inferior information: the direct update methods. These methods require the computation of only first derivatives of the cost function. Using the information obtained from the previous iterations, convergence towards the minimum is accelerated. In this study, we follow BFGS (Broyden-Fletcher-Goldfarb-Shanno) method which has been proved to be most effective in similar applications. We refer the interested reader to (Gill et al., 1981) for detailed derivations of this method.

14.3.2.7 A Case Study

The primary system is taken as a single-degree-of-freedom structure which is subjected to a wide band frequency load in the interval of $\omega \in [400,\ 1500]$ Hz. The DFVA is appended to it, and the resulting combined structure is shown in Figure 14.21. The primary system parameters are taken as $m_1 = 5.77$ kg, $k_1 = 251.132 \times 10^6$ N/m, and $c_1 = 1142.0$ kg/s. This system has a peak frequency at $\omega_{\text{peak}} = 1050$ Hz. The absorber mass to primary mass ratio is taken to be 3.9% ($m_a = 0.227$ kg).

The following strategy is used to determine the initial guess $\mathbf{X}_{abs}^0$. Considering the given physical parameters, the optimal passive absorber (i.e., $g = \tau = 0$) is found first: $\bar{k}_a = 9.5471 \times 10^6$ N/m and $\bar{c}_a = 359.20$ kg/s with the same objective function in mind (Equation (14.103)). Based on this

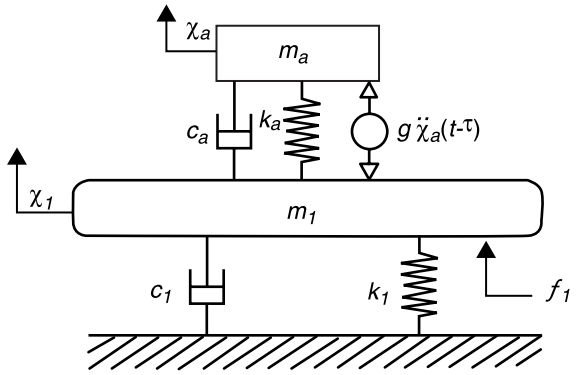

FIGURE 14.21 Implementation of a DFVA on a SDOF structure.

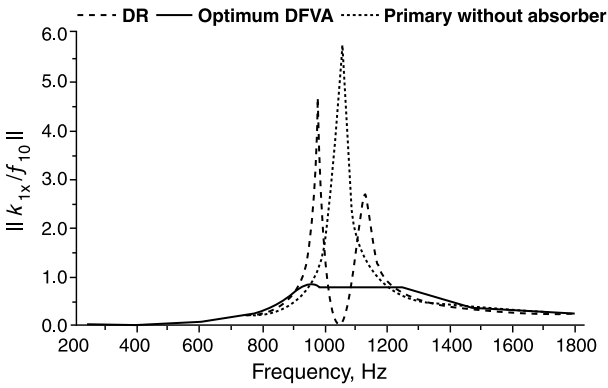

FIGURE 14.22 The frequency responses for different settings**.**

optimum passive absorber, the pure DR feedback gain and time delay are calculated at $\omega_c = 1050$ Hz: $g_c = 0.0550$ kg and $\tau_c = 1.1874 \times 10^{-3}$ sec. This setting of $[\bar{k}_a, \bar{c}_a, g_c, \tau_c]^T$ is taken as the starting vector: $\mathbf{X}^0_{abs} = [9.5471 \times 10^6, 359.20, 0.0550, 1.1874 \times 10^{-3}]^T$, for the following steps. The full scale optimization problem over $[k_a, c_a, g, \tau]^T \in \Re^4$ is handled to arrive at the *optimum DFVA* solution as:

$$\mathbf{X}^{opt}_{abs} = [k_a = 9.8014 \times 10^6,\ c_a = 35.4787,\ g = 0.0424,\ \tau = 0.7305 \times 10^{-3}]^T.$$

The frequency responses of the primary system alone, with DR (i.e., $\mathbf{X}^0_{abs}$), and with optimum DFVA are shown in Figure 14.22. All of these are obtained using the excitation force $f_1 = f_{10} \sin \omega t$. The optimum DFVA delivers better than 80% improvement over the DR in the vibration suppression at the first side frequency where the DR causes a substantial peak.

On the other hand, setting the absorber stiffness and damping (k_a, c_a) free during the optimization iterations offers a significant improvement as opposed to keeping them fixed. For open loop (passive) system ($g = 0$, $\tau = 0$) the characteristic roots are

$$s_{1,2} = -72.17 \pm j5921, s_{3,4} = -109.40 \pm j7348,\ f_1 = 942.4 \text{ Hz},\ f_2 = 1169.5 \text{ Hz} \quad (14.106)$$

The dominant roots for the corresponding optimum delayed feedback parameters are at

$$s^*_{1,2} = -406 \pm j5750,\ \text{for optimum DFVA case},\ g = 0.0424 \text{ kg},\ \tau = 0.7305 \text{ ms} \quad (14.107)$$

The respective damped natural frequencies at the dominant roots are calculated as

$$f_1^* = 915 \text{ Hz}, f_2^* = 1079 \text{ Hz}, f_3^* = 1294 \text{ Hz} \quad \text{for optimum DFVA case} \tag{14.108}$$

From Figure 14.22, it is clear that the peak frequencies are at about 930 Hz and 1090 Hz for optimum DFVA. The root placement is simpler to do than verifying the frequency response outlook for design purposes.

Acknowledgments

The presented study is supported in part by Connecticut Innovations Inc. (Grant No. 00Y14). Authors also wish to acknowledge the contributions of Mr. Chang Huang and Dr. Nader Jalili during their graduate work. Some parts of the discussions are reflective of their research work and referenced articles.

References

Abdel-Mooty M. and Roorda J., 1991, Time delay compensation in active damping of structures, *Journal of Engineering Mechanics,* 117, 2549.

Bapat, V. A. and Kumaraswamy, H. V., 1979, Effect of primary system damping on the optimum design of an untuned viscous dynamic vibration absorber, *Journal of Sound and Vibration*, 63, 469–474.

Carter, B. C., 1929, Improvements in or relating to damping or oscillation-checking devices, British Patent 337,466.

Den Hartog, J. P., 1938, Tuned pendulums as torsional vibration eliminators, *Stephen Timoshenko 60th Anniversary Volume*, Macmillan, London.

Den Hartog, J. P. and Ormondroyd J., 1928, Theory of the dynamic vibration absorber, *Transactions of the ASME*, APM-50-7, 11–22.

Den Hartog, J. P. and Ormondroyd, J., 1930, Torsional vibration dampers, *Transactions of ASME,* 52, 133–152.

DiDomenico, E., 1994. Passive vibration tuning with neural networks, *Proceedings of Smart Structures and Materials*, SPIE, 152–162.

Esmailzadeh, E. and Jalili, N., 1998, Optimal design of vibration absorbers for structurally damped Timoshenko beams, *ASME Journal of Vibration and Acoustics*, 120(4), 833–841.

Ezure, K. and Seto, K., 1994, Vibration control of two-degrees-of-freedom system using active dynamic absorber, *Transactions of the Japan Society of Mechanical Engineers, Part C*, 60, 788–795.

Filipovic, D. and Olgac, N., 1998, Torsional delayed resonator with speed feedback, *IEEE/ASME Transactions on Mechatronics*, 3(1), 67–72.

Frahm, H., 1911, Device for damping vibrations of bodies, United States Patent 989,958.

Franklin G. F., Powell J. D., and Emami-Naeini A., 1994, Feedback control of dynamic systems, Addison-Wesley, Reading, Massachusetts.

Gill, P. E., Murray, W., and Wright, M. H., 1981, *Practical Optimization*, Academic Press, New York.

Hertz, D., Jury, E.I., and Zeheb, E., 1984, Simplified analytic stability test for systems with commensurate time delays, *IEEE Proceedings, Part D*, 131(1), 52–56.

Hosek, M., 1997, Tunable torsional vibration absorber: The centrifugal delayed resonator, Ph.D. Dissertation, University of Connecticut, Storrs, Connecticut.

Hosek, M., 1998, Robust delay-controlled dynamic absorber, Doctoral dissertation, Czech Technical University in Prague.

Hosek, M., Elmali, H., and Olgac N., 1997a, A tunable torsional vibration absorber: The centrifugal delayed resonator, *Journal of Sound and Vibration*, 205(2), 151.

Hosek, M., Elmali, H., and Olgac N., 1997b, Centrifugal delayed resonator: Theory and experiments, *Proceedings of ASME Design Engineering Technical Conferences*, 16th Biennial Conference on Mechanical Vibration and Noise, Paper No. DETC97/VIB-3829, September 14–17, 1997, Sacramento, California.

Hosek, M., Elmali, H., and Olgac N., 1999, Centrifugal delayed resonator pendulum absorber, United States Patent No. 5934424.

Hosek, M. and Olgac, N., 1999, A single-step automatic tuning algorithm for the delayed resonator vibration absorber, *Proceedings of 1999 ASME International Mechanical Engineering Congress and Exposition*, Dynamic Systems and Control Division, 67, 157–164, November 14–19, Nashville, Tennessee.

Hosek, M., Olgac, N., and Elmali, H., 1999, The centrifugal delayed resonator as a tunable torsional vibration absorber for MDOF systems, *Journal of Vibration and Control*, 5, 2, 299–322.

Huang, C. and Olgac, N., *Proceedings, 2000 American Control Conference*, Chicago.

Inman, D. J., 1994, *Engineering Vibration*, Prentice-Hall, Englewood Cliffs, New Jersey.

Jacquot, R. G., 1978, Optimal dynamic vibration absorbers for general beams, *Journal of Sound and Vibration*, 60 (4), 535–542.

Jalili, N. and Olgac, N., 1999, Optimum delayed feedback vibration absorber for flexible beams, *Smart Structures*, NATO Science Series, Kluwer Academic, Amsterdam, 65, 237–246.

Jalili, N. and Olgac, N., 2000, A sensitivity study on optimum delayed feedback vibration absorber, *ASME Journal of Dynamic Systems, Measurement and Control*, 122, 2, 314–321.

Kolmanovskii, V.B. and Nosov, V.R., 1986, *Stability of Functional Differential Equations*, Academic Press, London.

Marshall, J. E., 1979, *Control of Time Delay Systems,* Peter Peregrinus Ltd., New York.

MATLAB/SIMULINK, version 5.3, Release R11, 1999, The MathWorks Inc., Natick, Massachusetts.

Nishimura, H., Nonami, K., Cui, W., and Shiba, A., 1993, H_∞ control of multi-degree-of-freedom structures by hybrid dynamic vibration absorber (experimental consideration of robustness and control performance), *Transactions of the Japan Society of Mechanical Engineers. Part C*., 59, 714–720.

Olgac, N., 1995, Delayed resonators as active dynamic absorbers, United States Patent 5,431,261.

Olgac, N., 1996, Single mass dual frequency fixed delayed resonator, United States Patent 5,505,282.

Olgac, N., Elmali, H., and Vijayan, S., 1996, Introduction to dual frequency fixed delayed resonator (DFFDR), *Journal of Sound and Vibration*, 189, 355–367.

Olgac, N., Elmali, H., Hosek, M., and Renzulli, M., 1995, High-frequency implementation of delayed resonator concept using piezoelectric actuators, *Proceedings of ACTIVE 95 — 1995 International Symposium on Active Control of Sound and Vibration*, 57–66.

Olgac, N., Elmali, H., Hosek, M., and Renzulli, M., 1997, Active vibration control of distributed systems using delayed resonator with acceleration feedback*, Journal of Dynamic Systems, Measurement and Control*, 119, 380–389.

Olgac, N. and Holm-Hansen, B., 1994, A novel active vibration absorption technique: Delayed resonator, *Journal of Sound and Vibration*, 176, 93–104.

Olgac, N. and Holm-Hansen, B., 1995a, Tunable active vibration absorber: The delayed resonator, *ASME Journal of Dynamic Systems, Measurement and Control*, 117, 513–519.

Olgac, N. and Holm-Hansen, B., 1995b, Design considerations for delayed-resonator vibration absorbers, *Journal of Engineering Mechanics*, 121, 80–89.

Olgac, N. and Hosek, M., 1995, Dual-frequency vibration absorption using delayed resonator with relative position measurement. *Proceedings of ASME Dynamic Systems and Control Division, ASME International Mechanical Engineering Congress and Exposition*, 2, 791, November 12–17, San Francisco, California.

Olgac, N. and Hosek, M., 1997, Active vibration absorption using delayed resonator with relative position measurement, *Journal of Vibration and Acoustics*, 119, 131–136.

Olgac, N. and Jalili, N., 1998, Modal analysis of flexible beams with delayed resonator vibration absorber: Theory and experiments, *Journal of Sound and Vibration*, 218(2), 307–331.

Orfanidis S. J., 1996, *Introduction to Signal Processing*, Prentice Hall, Englewood Cliffs, New Jersey.
Ormondroyd, J. and Den Hartog, J. P., 1928, The theory of the dynamic vibration absorber, *Transactions of ASME*, 50, 9–22.
Ozguven, H. N. and Candir, B., 1986, Suppressing the first and second resonance of beams by dynamic vibration absorbers, *Journal of Sound and Vibration*, 111(3), 377–390.
Puksand, H., 1975, Optimum conditions for dynamic vibration absorbers for variable speed systems with rotating and reciprocating unbalance, *International Journal of Mechanical Engineering Education*, 3, 145–152.
Rao, S. S., 1995, *Mechanical Vibrations*, 3rd ed., Addison-Wesley, New York.
Renzulli, M., 1996, An algorithm for automatic tuning of the delayed resonator vibration absorber, M.S. Thesis, University of Connecticut, Storrs.
Renzulli M. E., Ghosh-Roy R., and Olgac N., 1999, Robust control of the delayed resonator vibration absorber, *IEEE Transactions on Control Systems Technology*, 7(6), 683.
Rodellar J., Chung L. L., Soong T. T., and Reinhorn A. M., 1989, Experimental digital control of structures, *Journal of Engineering Mechanics*, 115, 1245.
Seto, K. and Fumishi, Y., 1991, A Study on Active Dynamic Absorber, ASME paper DE - Vol. 38.
Stepan, G., 1989, *Retarded Dynamical Systems Stability and Characteristic Functions*, Longman, London.
Sun, J. Q., Jolly, M. R., and Norris, M. A., 1995, Passive, adaptive, and active tuned vibration absorbers — a survey, *ASME Transactions, Special 50th Anniversary, Design Issue*, 117, 234–242.
Thomson, W. T., 1988, *Theory of Vibration with Applications*, Prentice Hall, Englewood Cliffs, New Jersey.
Thowsen A., 1981a, An analytic stability test for a class of time-delay systems, *IEEE Transactions on Automatic Control*, AC-26, 735.
Thowsen A., 1981b, The Routh-Hurwitz method for stability determination of linear differential-difference systems, *International Journal of Control*, 33, 991.
Thowsen A., 1982, Delay-independent asymptotic stability of linear systems, *IEE Proceedings*, 129, Part D, 73, 1982.
Valášek, M. and Olgac, N., 1999, New concept of active multiple frequency vibration suppression technique, *Smart Structures*, NATO Science Series, Kluwer Academic, 65, 373–382.
Warburton, G. B. and Ayorinde, E. O., 1980, Optimum absorber parameters for simple systems, *Earthquake Engineering and Structural Dynamics*, 8, 197–217.
Wilson, W. K., 1968, *Practical Solution of Torsional Vibration Problems,* Chapman and Hall, London.
Yang, B., 1991, Noncollocated control of damped string using time delay, *Proceedings, 1991 American Control Conference*, Boston.
Youcef-Toumi K. and Bobbett J., 1991, Stability of uncertain linear systems with time delay, *Journal of Dynamic Systems, Measurements, and Control*, 113, 558.
Youcef-Toumi K. and Ito O., 1990, A time delay controller for systems with unknown dynamics, *Journal of Dynamic Systems, Measurements, and Control*, 112, 133.
Zitek P., 1984, Stability criterion for anisochronic dynamic systems, *Acta Technica CSAV*, 4, 399.